COO - 1195-113

AN UPPER LIMIT ON THE DECAY RATE OF $K_L^0 \rightarrow \pi^+\pi^-\gamma$

BY

ROY CANNON THATCHER
B.S., Stanford University, 1961
M.S., University of Illinois, 1963

THESIS

Submitted in partial fulfillment of the requirements
for the degree of Doctor of Philosophy in Physics
in the Graduate College of the
University of Illinois, 1968

Urbana, Illinois

This research was supported in part by the U. S. Atomic Energy Commission
under contract AT(11-1)-1195.

DISCLAIMER

COO - 1195-113

AN UPPER LIMIT ON THE DECAY RATE OF $K_L^0 \rightarrow \pi^+\pi^-\gamma$

BY

ROY CANNON THATCHER
B.S., Stanford University, 1961
M.S., University of Illinois, 1963

THESIS

Submitted in partial fulfillment of the requirements
for the degree of Doctor of Philosophy in Physics
in the Graduate College of the
University of Illinois, 1968

Urbana, Illinois

This research was supported in part by the U. S. Atomic Energy Commission
under contract AT(11-1)-1195.

AN UPPER LIMIT ON THE DECAY RATE $K_L^o \rightarrow \pi^+\pi^-\gamma$

Roy Cannon Thatcher, Ph.D.

Department of Physics

University of Illinois, 1968

In the film from a spark chamber experiment on K_L^o decays performed in the 28° beam line of the ZGS at the Argonne National Laboratory, we undertook a search for the decay mode $K_L^o \rightarrow \pi^+\pi^-\gamma$. The charged decay products were momentum analyzed in a magnet and identified in a set of range-shower chambers on the basis of their behavior there. The position of the gamma ray conversion point in these chambers was compared with the position predicted on the hypothesis of $K_L^o \rightarrow \pi^+\pi^-\gamma$.

The $K_{\pi 3}$ provided almost the sole background as well as the normalization of our rate measurement. In 962 events with good gamma showers we found one event fitted the $\pi\pi\gamma$ hypothesis within our spacial resolution. However, the expected background was one event. This result corresponds to an upper limit on the decay rate $R(K_L^o \rightarrow \pi^+\pi^-\gamma) \leq 7.5 \times 10^3 \text{ sec}^{-1}$ at a confidence level of 90%. The result is compared with the predictions of various theoretical models. The possible connections to other decay processes ($K^{\pm} \rightarrow \pi^{\pm}\pi^o\gamma$, $K_L^o \rightarrow \pi^o\pi^o\gamma$, $K_S^o \rightarrow \pi^+\pi^-\gamma$) and the feasibilities of CP invariance tests are discussed.

ACKNOWLEDGMENTS

The author is deeply grateful to Professor Albert Wattenberg whose help and guidance were invaluable and whose great drive and love of physics have been inspiring. He would also like to thank:

Professor A. Abashian for help and encouragement in all phases of this work;

Dr. R. J. Abrams who designed and supervised the construction of much of the equipment used in this experiment;

Dr. R. E. Mischke whose thesis experiment produced the film used in this experiment and whose efforts in all areas, particularly programming, were very important;

Dr. L. J. Verhey whose aid in analysis of detection efficiency was invaluable;

Prof. J. H. Smith, Dr. B. M. K. Nefkens and Dr. D. W. Carpenter for their advice and help;

Mrs. Pat Martin whose help and encouragement was inestimably valuable, and also the scanners she supervised;

Mrs. Doris Bermingham for typing the thesis;

the United States Atomic Energy Commission for the financial support of this experiment.

This work is dedicated to Aileen.

TABLE OF CONTENTS

I. INTRODUCTION

At the present time there is great interest in studying CP violation in K-meson systems. CP conservation forbids the decays $K_2^o \to \pi^+\pi^-$ and $K_2^o \to \pi^o\pi^o$. The observation of the former[1] of these two decay modes led to a rash of theories many of which struggled valiantly to "save" CP. But CP was not to be saved. The observation of interference between $K_S^o \to \pi^+\pi^-$ and $K_L^o \to \pi^+\pi^-$ can be explained only by the violation of CP. Since then CP violation has been observed in $K_L^o \to \pi^o\pi^o$ [2] in the $K_L^o \to \pi^\pm \ell^\mp \nu$ [3] where it shows up as a small charge asymmetry.

Whereas the existence of CP violation is now well established, one does not yet know precisely where the violation occurs. Although it is only in weak decays that the small CP violating effects have been seen, the CP violation could be due to the strong interaction,[4] or to the electromagnetic interaction[5] or to the weak interaction[6] or to a combination of all of these. It might also be due to a new interaction.[7] To pin down the location and nature of the CP violation, several different reactions must be observed which manifest this violation. The radiative decay of the charged and neutral K-mesons have become of great interest as a possible test of theoretical proposals for understanding CP violation.

This thesis is a report on a spark chamber experiment performed at the Argonne National Laboratory's ZGS to search for the

decay mode $K_L^o \to \pi^+\pi^-\gamma$. There are two CP violation effects which have been proposed as possibly showing up in this decay.

Lee and Wu[8] pointed out that if there are large C and T violations in the electromagnetic interactions, these could manifest themselves as a small (1%) asymmetry in the π^+, π^- energy distribution. This is about 300 times the asymmetry one could expect if CP violation is entirely in the weak interactions. But in view of the small upper limit on the branching ratio of $K_L^o \to \pi^+\pi^-\gamma$, there is little hope of seeing such an effect in this decay.

Sehgal and Wolfenstein[9] have pointed out that one might get strong interference between $K_L^o \to \pi^+\pi^-\gamma$ and $K_S^o \to \pi^+\pi^-\gamma$ if a CP violation is associated with the interactions involved in the emission of the photon. The present experimental data on $K_S^o \to \pi^+\pi^-\gamma$ are consistent with inner bremsstrahlung. The calculated rate for this process for a gamma ray energy $E_\gamma \geqslant 50$ MeV is rate $(K_S^o \to \pi^+\pi^-\gamma) = 1.6 \times 10^7$ sec^{-1}. This is 4×10^4 times greater than the upper limit on the rate for $(K_L^o \to \pi^+\pi^-\gamma)$ which we obtained in this experiment. Interference effects are most marked between equal amplitudes; therefore the low rate for the K_2^o radiative decay we have observed makes the experimental test of Sehgal and Wolfenstein unfeasible at the present state of the art.

Several models have been used to calculate the rate for $K_L^o \to \pi^+\pi^-\gamma$. One can also relate the magnetic dipole contributions

to direct emission for $K_L^o \to \pi^+\pi^-\gamma$ and for $K^+ \to \pi^+\pi^o\gamma$ if one assumes an extension of the $\Delta I = 1/2$ rule proposed by D. Cline. These will be discussed in the next section.

II. THEORETICAL CALCULATION OF THE DECAY $K_L^o \to \pi^+\pi^-\gamma$

The decay $K_L^o \to \pi^+\pi^-\gamma$ can proceed by direct emission of the photon or by inner bremsstrahlung. However inner bremsstrahlung is small because the $K_L^o \to \pi^+\pi^-$ mode violates CP invariance.* We can expect that those direct processes which conserve CP should dominate the radiative decay.

The quantum numbers of the $\pi^+\pi^-\gamma$ final state for the first terms in the multipole expansion are shown in Table 1. Since K_L^o can be assumed to be very nearly an eigenstate of CP with eigenvalue -1, the CP conserving processes are seen to be magnetic dipole and electric quadrupole emission.

At the present state of the art our attempts to calculate the $K_L^o \to \pi^+\pi^-\gamma$ decay rate should be viewed as estimates rather than precise computations. In all treatments to be discussed here the theorists neglect the electric quadrapole contribution to the direct emission process and compute only the magnetic dipole term. The dipole term is easier to calculate. As $\ell_{\pi\pi} = 1$ for the M_1 transition and as $\ell_{\pi\pi} = 2$ for the E_2 transition the dipole should be bigger than the quadrupole from angular momentum considerations alone.

---

*One can estimate the rate for internal bremsstrahlung by itself: $R_{K_L^o \to \pi^+\pi^-\gamma}(\text{I.B.}) \sim R_{K_L^o \to \pi^+\pi^-} \times \alpha$, the fine structure constant. This gives a branching ratio estimate of $R(\text{I.B.})_{K_L^o \to \pi^+\pi^-\gamma} / R(K_L^o \to \text{all}) \sim 10^{-5}$.

Table 1

Quantum Numbers of the Final State for

$K_L^o \rightarrow \pi^+\pi^-\gamma$

	M1	E1	M2	E2
$\ell_{\pi^+\pi^-}$	1	1	2	2
j_γ	1	1	2	2
$I_{\pi\pi}$	1	1	0,2	0,2
$C_{\pi\pi\gamma}$	1	1	-1	-1
$P_{\pi\pi\gamma}$	-1	+1	-1	+1
$CP_{\pi\pi\gamma}$	-1	+1	+1	-1

$$C_{\pi\pi\gamma} = (-1)^{\ell\pi^+\pi^-}(-1) \text{ photon}$$

$$P_{\pi\pi\gamma} = \begin{cases} (-1)^{\ell\pi^+\pi^-}(-1)^{j\gamma+1} & \text{Magnetic Multipoles} \\ (-1)^{\ell\pi^+\pi^-}(-1)^{j\gamma} & \text{Electric Multipoles} \end{cases}$$

Estimates of the magnetic dipole term to the rate have been made by D. Cline, Pepper and Ueda, Oneda, Kim and Korff, and Lai and Young. The basic ideas of each of these calculations are outlined in the paragraphs which follow and their results are summarized in Table 2 at the end of the chapter.

D. Cline[10] has calculated an upper limit for the M1 direct emission assuming a $|\Delta I| = 1/2$ rule in which the photon is ignored in computing the isospin of the final state. There is no a priori justification for the assumption of such a rule but it is an interesting speculation.

Subtracting the calculated inner bremsstrahlung from the experimental limit for $K^+ \to \pi^+\pi^o\gamma$, Cline obtains an upper limit on the rate due solely to M1 radiation.

$R_+(K^+ \to \pi^+\pi^-\gamma;\ M1) \leqslant 3 \times 10^4\ \text{sec}^{-1}$. Using the Wigner-Ekhart theorem and neglecting meson mass differences, he finds

$$\frac{R_2(M1)}{R_+(M1)} = \frac{R(K_L^o \to \pi^+\pi^-\gamma,\ M1)}{R(K^+ \to \pi^+\pi^o\gamma,\ M1)} = \left| \frac{\sqrt{2}\,\Delta_3 - 1}{1 + \Delta_3/\sqrt{2}} \right|^2 \qquad (1)$$

where Δ_3 is the ratio of $|\Delta I| = 3/2$ amplitude to that for $|\Delta I| = 1/2$. Cline's $|\Delta I| = 1/2$ rule is invoked by setting $\Delta_3 = 0$ in Eq. (1).

$$R_2(M1) = R_+(M1) \qquad (2)$$

$$\frac{R_2(M1)}{R(\text{all } K_L^o \text{ decays})} \leqslant 2 \times 10^{-3}$$

Pepper and Ueda[11] consider two different mechanisms and estimate the contribution of each to $K_L^o \to \pi^+\pi^-\gamma$. The first of these is a model generalized from the Cabibbo-Gatto[12] interaction and is based on a strong kaon-pion vertex, a two particle intermediate state and a weak $|\Delta I| = 1/2$ interaction. This model gives a very small branching ratio

$$\frac{\text{Rate } (K_L^o \to \pi^+\pi^-\gamma)}{\text{Rate } (K_L^o \to \text{all})} < 3 \times 10^{-8}$$

Since this model gives a much smaller branching ratio than inner bremsstrahlung, we shall ignore it in all further discussion.

The second model they consider is the boson pole model.[13-15] Here one assumes that the strangeness changing vertex can be attributed to an effective two-point kaon pseudo-scalar meson $\Delta I = 1/2$ weak interaction. The diagrams calculated are shown in Fig. 1.

The Lagrangian used by Pepper and Ueda has the $\Delta I = 1/2$ rule implicit in its coupling constants;

$$\mathcal{L} = - f_{K^+\pi^+} m_\pi^2 K_2^o \pi^o + f_{K\eta} m_\pi^2 K_2^o \eta$$

$$+ \frac{\lambda}{m_\pi} \varepsilon_{\mu\nu\sigma\rho} \partial_\mu A_\nu \partial_\sigma \rho_\rho^+ \pi + \frac{\lambda}{m_\pi} \varepsilon_{\mu\nu\sigma\rho} \partial_\mu A_\nu \partial_\sigma \rho_\rho^o \pi_o$$

$$+ \frac{\lambda_3}{m_\pi} \varepsilon_{\mu\nu\sigma\rho} \partial_\sigma \rho_\rho^o \eta + f_{\rho\pi\pi} \rho \cdot \pi \times \partial_\mu \pi$$

Figure 1. The Feynman diagrams used by Pepper and Ueda in calculating the direct emission contribution to $K_L^o \rightarrow \pi^+\pi^-\gamma$.

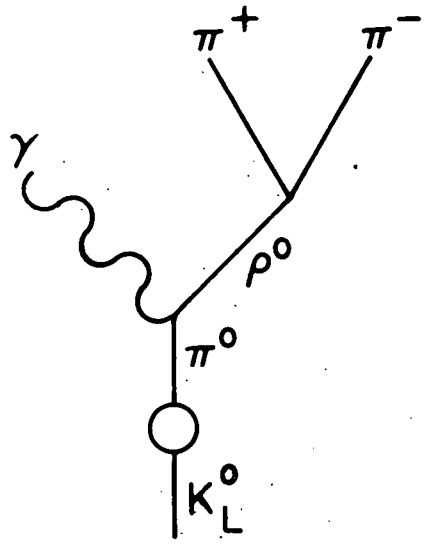

(a)

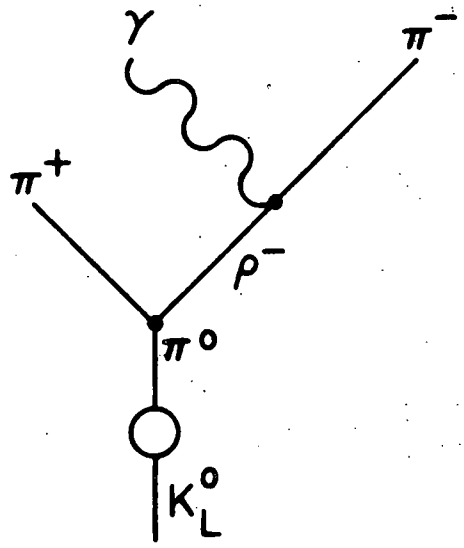

(b)

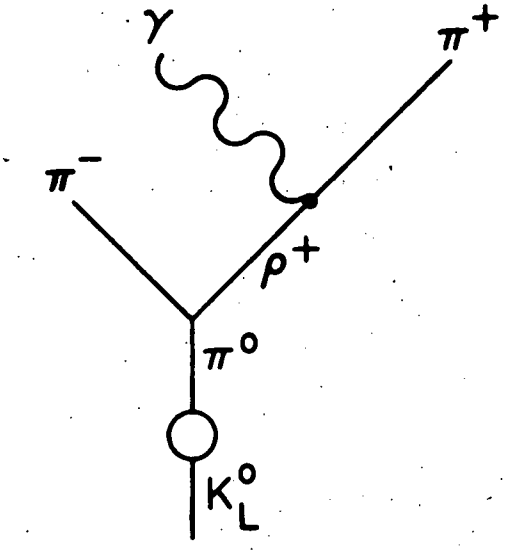

(c)

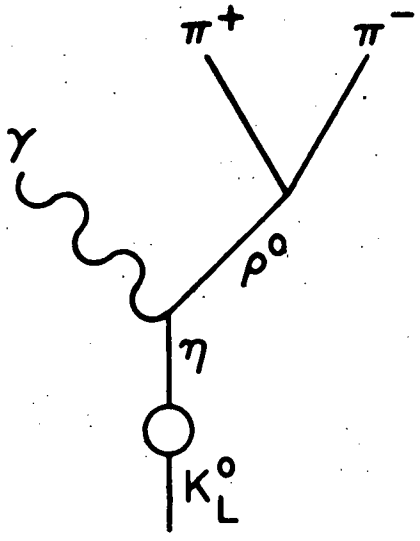

The pion pole amplitudes can interfere with the eta pole terms so the relative sign of $f_{K^+\pi^+}$ and $f_{K\eta}$ becomes important. A unitary symmetry generalization of the $|\Delta I| = 1/2$ rule gives $f_{K^+\pi^+}/f_{K\eta} = -6$ and $\lambda_3/\lambda = 3$. This gives destructive interference. Although mass differences may shift the magnitudes of these ratios, it is hoped that the sign is right. In this way Pepper and Ueda obtain for the direct process

$$\frac{\text{Rate}\ (K_L^o \to \pi^+\pi^-\gamma)}{\text{Rate}\ (K_L^o \to \text{all})} = 6.7 \times 10^{-4}. \qquad (4)$$

This result is rather uncertain since the $f_{K^+\pi^+}$ and $f_{K\eta}$ coupling constants are known only to an order of magnitude.

Oneda, Kim and Korff estimated the decay rate using the pseudoscalar meson pole approximation and a current-current type of interaction which transforms like a member of an SU(3) octet.[17-24] The Feynman diagrams calculated are shown in Fig. 2. Note that Oneda, Kim and Korff use the same diagrams as Pepper and Ueda plus others involving $K^{\pm}$ and $K_o^* - \overline{K}^{o*}$. The SU(3) generalized Lagrangian for $\rho\pi\gamma$ type vertices is

$$\begin{aligned}\mathcal{L}_{VP\gamma} = i\lambda_{\rho\pi\gamma}\, \varepsilon_{\alpha\beta\gamma\delta}\, \partial_\alpha A_\beta \Big\{ & \partial_\gamma \pi^o \rho_\delta^o + \partial_\gamma \pi^- \rho_\delta^- \\ & + \partial_\gamma K^- P_\delta^+ + \sqrt{3}\ \partial_\gamma \eta^o \rho_\delta^o + \partial_\gamma K^- K_\delta^{*+} + \partial_\gamma K^+ K_\delta^{*-} \\ & - 2\partial_\gamma K^o \overline{K^o}_\delta^{\,*} - 2\partial_\gamma \overline{K^o} K_S^{*o} + \ldots \Big\}\end{aligned} \qquad (5)$$

Figure 2. The Feynman diagrams used by Oneda, Kim and Korff in calculating the direct emission contribution to $K_L^o \rightarrow \pi^+\pi^-\gamma$.

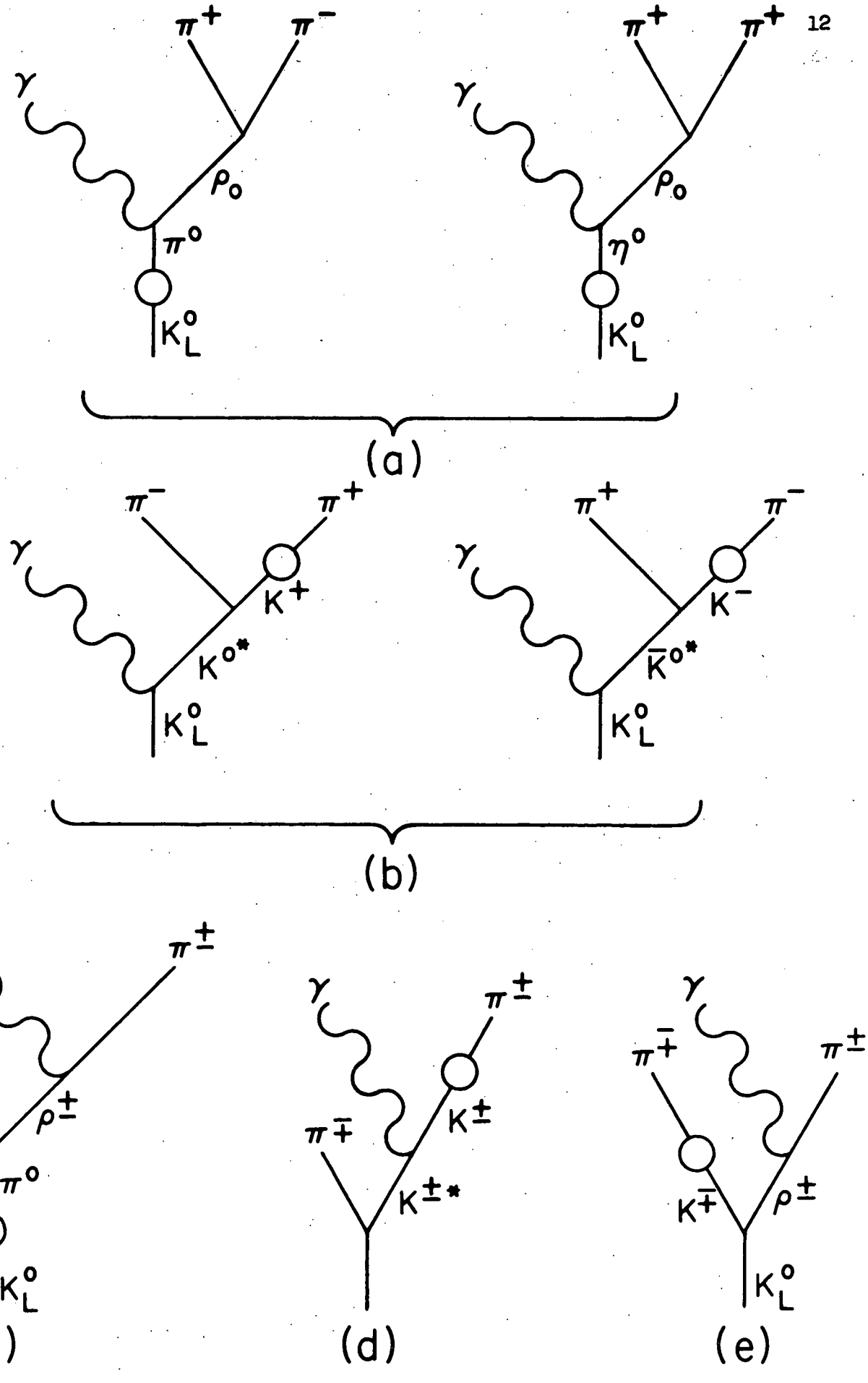
γ
π+
π−
ρ0
π0
K0L
(a)
γ
π+
π+
ρ0
η0
K0L
γ
π−
π+
K+
K0*
K0L
(b)
γ
π+
π−
K−
K̄0*
K0L
γ
π±
π∓
ρ±
π0
K0L
(c)
γ
π±
π∓
K±
K±*
(d)
γ
π±
π∓
K∓
ρ±
K0L
(e)

The coupling constant $\lambda_{\rho\pi\gamma}$ is estimated from the $\pi^o \to 2\gamma$ decay rate to be

$$\lambda^2_{\rho\pi\gamma} \simeq \frac{1.3 \times 10^{20}\ \text{sec}^{-1}}{m_\pi^3} .$$

From the width of the ρ meson (taken to be 100 MeV) $G_{\rho\pi\pi}$ is given approximately by

$$\frac{(G_{\rho\pi\pi})^2}{4\pi} = 0.50 .$$

The amplitude for the diagrams in Fig. 2a takes the form

$$M = -4\left(\frac{m_k^2}{m_\pi^2 - m_k^2} + \frac{m_k^2}{m_\eta^2 - m_k^2}\right) f_w \lambda_{\pi\gamma} G_{\rho\pi\pi} \varepsilon_{\mu\nu\lambda\beta}$$

$$\times k_\mu e_\nu P^+_\lambda P^-_\beta \frac{1}{m_\rho^2 + (p^+ + p^-)^2}$$

where k, p^+ and p^- are the four momenta of the photon, the π^+ and the π^- mesons, respectively. e_ν is the polarization vector of the photon.

Exact SU(3) is used to obtain the relations between the coupling constants

$$(f_w)_{K_2^o \to \pi^o} = 3^{-1/2} (f_w)_{K_2^o \to \eta^o}$$

$$\lambda_{\rho^o\pi^o\gamma} = 3^{-1/2} \lambda_{\rho^o\eta^o\gamma}$$

The coupling constant $\lambda_{\rho\pi\gamma}$ is estimated from the $\pi^o \to 2\gamma$ decay rate to be

$$\lambda^2_{\rho\pi\gamma} \simeq \frac{1.3 \times 10^{20}\ \text{sec}^{-1}}{m_\pi^3} .$$

From the width of the ρ meson (taken to be 100 MeV) $G_{\rho\pi\pi}$ is given approximately by

$$\frac{(G_{\rho\pi\pi})^2}{4\pi} = 0.50 .$$

The amplitude for the diagrams in Fig. 2a takes the form

$$M = -4\left(\frac{m_k^2}{m_\pi^2 - m_k^2} + \frac{m_k^2}{m_\eta^2 - m_k^2}\right) f_w \lambda_{\rho\pi\gamma} G_{\rho\pi\pi} \varepsilon_{\mu\nu\lambda\beta}$$

$$\times k_\mu e_\nu P^+_\lambda P^-_\beta \frac{1}{m_\rho^2 + (p^+ + p^-)^2}$$

where k, p^+ and p^- are the four momenta of the photon, the π^+ and the π^- mesons, respectively. e_ν is the polarization vector of the photon.

Exact SU(3) is used to obtain the relations between the coupling constants

$$(f_w)_{K_2^o \to \pi^o} = 3^{-1/2} (f_w)_{K_2^o \to \eta^o}$$

$$\lambda_{\rho^o\pi^o\gamma} = 3^{-1/2} \lambda_{\rho^o\eta^o\gamma}$$

The other Feynman amplitudes are constructed similarly. Assuming that the weak coupling constant, f_w, depends only weakly on the external momentum q^2, then the rate for the direct process is found to be

$$R(K_L^o \to \pi^+\pi^-\gamma) = 0.51 \times (1 \pm 0.5) \times 10^3 \text{sec}^{-1}$$

and the branching ratio is

$$\frac{R(K_L^o \to \pi^+\pi^-\gamma)}{R(K_L^o \to \text{all})} = 2.9 \times (1 \pm 0.5) \times 10^{-5} \tag{7}$$

When Oneda, Kim and Korff include ω-φ mixing, they obtain a larger rate and branching ratio:

$$R(K_L^o \to \pi^+\pi^-\gamma) = (2\text{-}3) \times (1 \pm 0.5) \times 10^3 \text{sec}^{-1}$$

$$\frac{R(K_L^o \to \pi^+\pi^-\gamma)}{R(K_L^o \to \text{all})} = (1.14 - 1.70) \times (1 \pm 0.5) \times 10^{-4} \tag{8}$$

Lai and Young[25] used the method of current algebras to calculate the ratio of the rate for the direct CP conserving process for $K_L^o \to \pi^+\pi^-\gamma$ to the rate for $K_L^o \to \gamma\gamma$. Since the rate for $K_L^o \to \gamma\gamma$ has been experimentally measured, this gives them a prediction on the absolute rate of $K_L^o \to \pi^+\pi^-\gamma$. In their notation $J_\mu^i(x) = V_\mu^i(x) + A_\mu^i(x)$ is the sum of the vector and axial vector currents and the superscript i is an SU(3) index. Using the PCAC hypothesis, $\partial_\mu A_\mu^i(x) = C_\pi^i \varphi^i(x) i = 1,2,3$ and assuming the $|\Delta I| = 1/2$ rule, they get the CP conserving

direct amplitude

$$M_1(K_L^o \to \pi^+\pi^-\gamma) = 2\pi^{-3/2}(2k_o)^{-1/2} e_{ch} \frac{m_\pi^4}{c_\pi^2} (p-q)_\mu M_\mu^3(p+q,k) \quad (9)$$

where p, q, and k refer to the four momenta of the π^+, π^- and photon respectively, and e_{ch} is the electronic charge. M_μ^3 is defined by

$$ie\, M_\mu^3(p+q,k) = (2\pi)^{3/2}(2k_o)^{1/2} \int d^4x\, e^{-i(p+q)} \cdot x \langle \gamma, ke | T \{V_\mu^3(x), H_w(0)\} | K_2^o \rangle \quad (10)$$

where $H_w(0)$ is the weak Hamiltonian responsible for non-leptonic decays.

For $K_2^o \to \gamma\gamma$ the decay amplitude is given by

$$M(K_2^o \to \gamma\gamma) = (2\pi)^{-3/2}(2k'_o)^{-1/2} \langle \gamma k'e', \gamma ke | H_w(0) | K_2^o \rangle \quad (11)$$

$$= ie\, \varepsilon_\mu^1 \int d^4x e^{-ik'\cdot x} \langle \gamma k\varepsilon | T \{V_\mu^{em}(x), H_w(0)\} | K_2^o \rangle$$

where k, k', e and e' are the four-momenta and polarization of the two photons, and $e_{ch}V_\mu^{em} = e_{ch}(V_\mu^3 + \frac{1}{\sqrt{3}} V_\mu^8)$ is the electromagnetic current operator. Then by covariance they write this as

$$M(K_2^o \to \gamma\gamma) = (2\pi)^{-3/2}(2k_o)^{-1/2}(ie_{ch})^2 M^{em} \varepsilon_{\mu\nu\alpha\beta} e'_\mu e_\nu k'_\alpha k_\beta \quad (12)$$

$$+ \text{CP-noninvariant term}$$

where M^{em} is the CP conserving part of the K_2^o $\gamma\gamma$ form factor. The

CP-violating term is neglected since it should be nearly three orders of magnitude smaller.

Comparing Eqs. (10), (11), and (12) and using the definition of V_μ^{em}, Lai and Young write

$$M_\mu^3(p+q,\ k) = \lambda\ M^{em}\ \varepsilon_{\mu\nu\alpha\beta}\ e\ (p+q)_\alpha\ k_\beta \tag{13}$$

where the factor λ (correcting for the contribution of the isoscalar part of the photon) is calculated from SU(3) to be

$$\lambda = 1/2 + \frac{1}{\sqrt{3}} \cdot \frac{3}{2}$$

Combining Eqs. (9) and (13) gives

$$M_1(K_2^o \to \pi^+\pi^-\gamma) = (2\pi)^{-3/2}(2k_o)^{-1/2}\ \frac{2m_\pi^4}{c_\pi^2}\ e\lambda\ M^{em}\ \varepsilon_{\mu\nu\alpha\beta} p_\mu e_\nu q_\alpha k_\beta$$

and assuming a constant form factor M^{em}, the branching ratio of $R_1(K_2^o \to \pi^+\pi^-\gamma)$ and $R\ (K_2^o \to 2\gamma)$ is

$$\frac{R_1(K_2^o \to \pi^+\pi^-\gamma)}{R\ (K_2^o \to 2\gamma)} = \frac{m_\pi^8\ \lambda^2}{2\pi\alpha c_\pi^4\ m_k^2} \int_o^{\frac{m_K^2 - 4m_\pi^2}{2m_K}} k^3 dk \left(1 - \frac{4m_K^2}{m_K^2 - 2m_K k}\right)^{1/2}$$

$$\times \left\{\frac{2}{3}(m_K^2 - 2m_K k - 2m_\pi^2) + \frac{m_\pi^4}{m_K^2 - 2m_K k}\right\} \tag{14}$$

where $\alpha = e^2/4\pi$, $C_\pi = \sqrt{2}\ m_N\ F_A / g_{NN\pi}$, and $g_{NN\pi}^2/4\pi \simeq 14.6$, $F_A = 1.18$. Upon substitution and integration

$$R_1(K_2^o \to \pi^+\pi^-\gamma)/R(K_2^o \to 2\gamma) \simeq 0.14 \tag{15}$$

Using the experimental value for the $K_L^o \to \gamma\gamma$ rate,[2,26]

$$\frac{R(K_L^o \to 2\gamma)}{R(K_2^o \to \text{all})} \simeq (7.4 \pm 1.6) \times 10^{-4} ,$$

they obtain for the direct process the prediction

$$\frac{R_1(K_2^o \to \pi^+\pi^-\gamma)}{R(K_2^o \to \text{all modes})} \simeq (10 \pm 2.2) \times 10^{-5} \tag{16}$$

Since all these estimates are rather small, it now becomes worthwhile to consider inner bremsstrahlung[27,28] with some precision. For this process the matrix element is given by

$$M_B(K_2^o \to \pi^+\pi^-\gamma) = (2\pi)^{-3/2}(2k_o)\, e\, M(K_2^o \to \pi^+\pi^-) \times \left(\frac{\vec{p}\cdot\vec{e}}{\vec{p}\cdot\vec{k}} - \frac{\vec{q}\cdot\vec{e}}{\vec{q}\cdot\vec{k}}\right) \tag{17}$$

where $M(K_2^o \to \pi^+\pi^-)$ is the matrix element for the CP violating decay $K_2^o \to \pi^+\pi^-$. The branching ratio of this bremsstrahlung process in $K_2^o \to \pi^+\pi^-\gamma$ to the decay $K_2^o \to \pi^+\pi^-$ is then given by

$$\frac{R_B(K_2^o \to \pi^+\pi^-\gamma)}{R(K_2^o \to \pi^+\pi^-)} = \frac{\alpha}{\pi(1-4m_K^2/m_K^2)^{1/2}} \int_{E_\gamma}^{\frac{m_K^2 - 4m_\pi^2}{2m_K}} \frac{dk}{k}\left(1 - \frac{2k}{m_K}\right) \times \left\{\left(1 - \frac{2m_\pi^2}{m_K^2 - 2m_K k}\right) \ln \left(\frac{1+\sqrt{1 - \frac{4m_\pi^2}{m_K^2 - 2m_K k}}}{1-\sqrt{1 - \frac{4m_\pi^2}{m_K^2 - 2m_K k}}}\right) - \sqrt{1 - \frac{4m_\pi^2}{m_K^2 - 2m_K k}}\right\} = \begin{cases} 1.1\,\% & E_\gamma \geq 10 \text{ MeV} \\ 0.26\% & E_\gamma \geq 50 \text{ MeV} \end{cases} \tag{18}$$

where E_γ is the energy of the photon in the radiative decay.

Comparing with the experimental branching ratio for $K_2^o \to \pi^+\pi^-$ [26]

$$\frac{R(K_2^o \to \pi^+\pi^-)}{R(K_2^o \to \text{all})} = (1.53 \pm 0.007) \times 10^{-3}$$

we find for the bremsstrahlung process

$$\frac{R(K_2^o \to \pi^+\pi^-\gamma)}{R(K_2^o \to \text{all modes})} \simeq \begin{cases} 1.69 \times 10^{-5} & E_\gamma \geq 10 \text{ MeV} \\ 0.4 \times 10^{-5} & E_\gamma \geq 50 \text{ MeV} \end{cases} \quad (19)$$

The branching ratios calculated from the various models are summarized in the Table II-2.

Table 2

Theorist	Description of Model	Rate $(K_L^o \to \pi^+\pi^-\gamma)$	$\frac{\text{Rate}(K_L^o \to \pi^+\pi^-\gamma)}{\text{Rate}(K_L^o \to \text{All})}$
D. Cline	$\Delta I = 1/2$; calculated value of inner bremsstrahlung is subtracted from experimental value.	$3 \times 10^4 \text{sec}^{-1}$	$\leq 2 \times 10^{-3}$
Pepper and Ueda	Boson pole approximation; $\Delta I = 1/2$ to get $K_2^o - \pi^o$ coupling constant; Unitary symmetry generalization of $\Delta I = 1/2$ to get sign of η-π interference	$1.2 \times 10^4 \text{ sec}^{-1}$	6.7×10^{-4}
Oneda, Kim and Korff	Boson pole approximation; SU(3) generalize $\Delta I = 1/2$ is built in; coupling constants from SU(3) and model for $\pi^o \to \gamma\gamma$; ω/φ mixing	$(2\text{-}3) \times (1\pm0.5) \times 10^3 \text{sec}^{-1}$	$(1.14\text{-}1.70) \times (1\pm0.5) \times 10^{-4}$
Oneda, Kim and Korff	Same as before but with no ω/φ mixing.	$0.51 \times (1 \pm 0.5) \times 10^3 \text{sec}^{-1}$	$2.9 \times (1\pm0.5) \times 10^{-5}$
Lai and Young	Current algebra, PCAC, experimental rate $(K_L^o \to \gamma\gamma)$	$(1.7 \pm .4) \times 10^3 \text{ sec}^{-1}$	$(10 \pm 2.2) \times 10^{-5}$
	Inner bremsstrahlung	$2.88 \times 10^2 \text{sec}^{-1}$ $E_\gamma \geq 10$ $.68 \times 10^2 \text{sec}^{-1}$ $E_\gamma \geq 50$	1.69×10^{-5} $E_\gamma \geq 10$ MeV $.4 \times 10^{-5}$ $E_\gamma \geq 50$ MeV

III. EXPERIMENTAL DETAILS

The experiment was performed in the 31° neutral beam of the ZGS at the Argonne National Laboratory. See Fig. 3 for a schematic of the beam layout. Circulating protons of momentum 11.6 GeV/c struck one or two internal targets just upstream of the L3 straight section of the machine. Target A was a multiple-pass target of 1/8" x 1/4" x 1/4" beryllium. Target C was of 1/8" x 1/4" x 3.85" copper. Fifty rolls of film were taken with target A only, 180 rolls with both A and C targets and 18 rolls with target C only.

During the experiment the beam spill varied from 50 to 400 milliseconds and the beam intensity from 1×10^{10} to 5×10^{11} protons on target per machine pulse. Four collimators were used with the last collimator providing the defining aperture. This 48" long brass collimator had a tapered opening which was 1.78" high by 1.25" wide at a point 48' from target.

Gamma rays in the beam were attenuated by two inches (10 radiation lengths) of lead just upstream of the first collimator (see Fig. 3). The electrons and positrons produced in the lead as well as other charged particles already in the beam were swept out by a bending magnet (BM-105) between the second and third collimators. The beam reaching our apparatus consisted mainly of neutrons and K_2^o mesons.

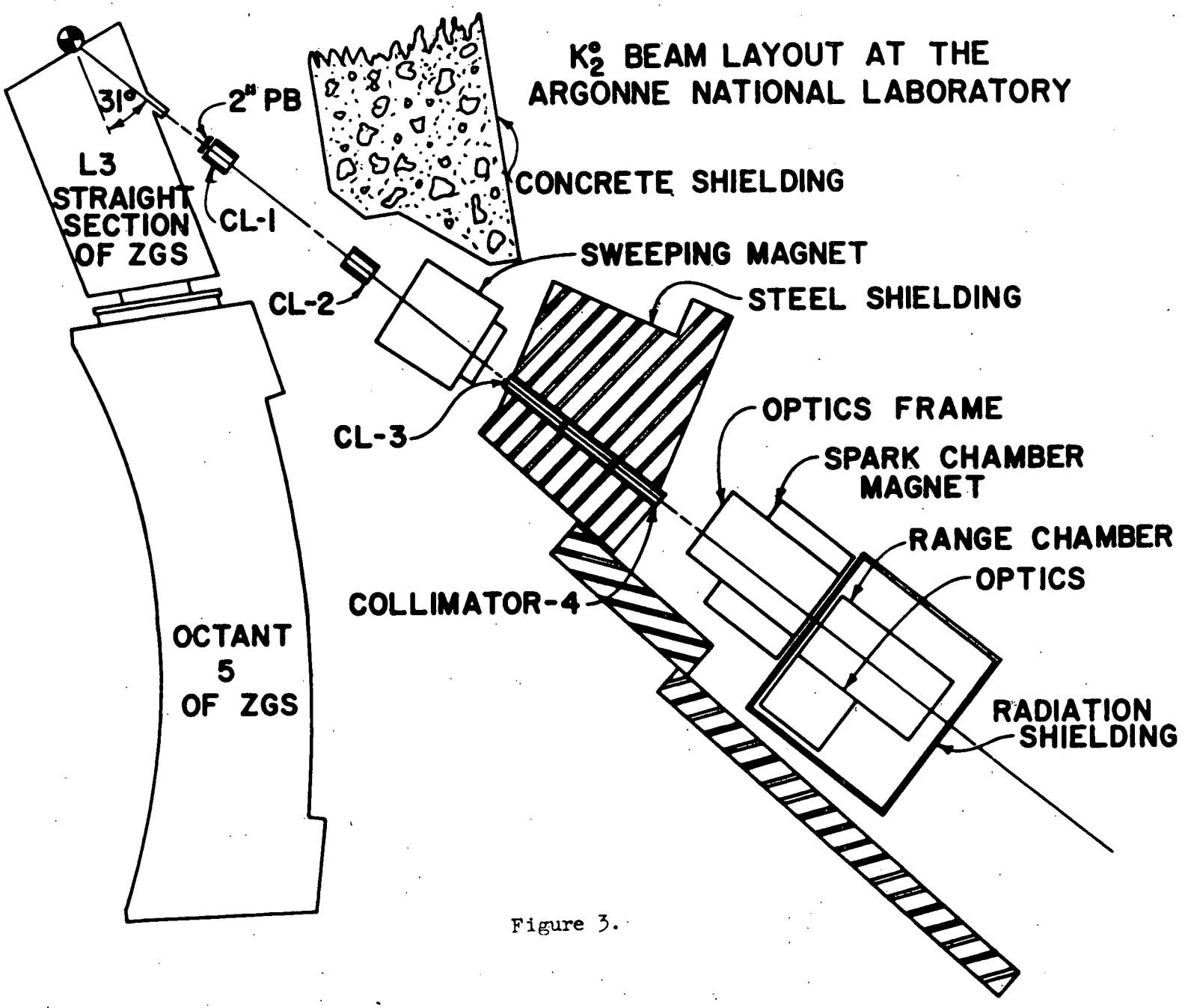
K_2° BEAM LAYOUT AT THE ARGONNE NATIONAL LABORATORY
31°
2" PB
L3 STRAIGHT SECTION OF ZGS
CL-1
CONCRETE SHIELDING
SWEEPING MAGNET
CL-2
STEEL SHIELDING
CL-3
OPTICS FRAME
SPARK CHAMBER MAGNET
RANGE CHAMBER
OPTICS
COLLIMATOR-4
OCTANT 5 OF ZGS
RADIATION SHIELDING

Figure 3.

The apparatus can be divided roughly into two parts. (See Fig. 4):

1) scintillation counters for the detection of the decay and thin walled spark chambers in a magnetic field for the measurement of the momenta of the charged decay products,

2) spark chambers with 1/8" thick aluminum plates for the identification of the decay products and hence the decay mode.

To make sure that events were decays and not interactions all decays were required to originate from within a vacuum pipe built into the first of the two magnet spark chambers. The vacuum pipe was an oval tube of thin stainless steel with .005" mylar end and side walls. The vacuum pipe was 12" long and roughly 57' from the target.

The magnet spark chambers were made of .001" aluminum foil plates and each had twelve 1/4" gaps at intervals of 1.25". In the first nine foils of the upstream chamber there was a three inch by four inch rectangular hole for the vacuum pipe. Of the 24 gaps the last 22 were photographed through the slotted upper pole face of the magnet. The walls between the two chambers were of .003" mylar bonded to .002" of aklar with Eastman 910. Aklar was selected for its low permeability to water vapor. The back wall of the back chamber was of 5/8" aluminum.

The magnet in which the chambers were situated had a 14" high gap and produced a field with an average vertical component of 9.78

Figure 4. ARRANGEMENT FOR $K_L^0 \rightarrow \pi^+\pi^-\gamma$ EXPERIMENT

COINCIDENCE $\bar{A}_\alpha \bar{A}_\beta M_1 M_2 \Omega_1 \Omega_2$

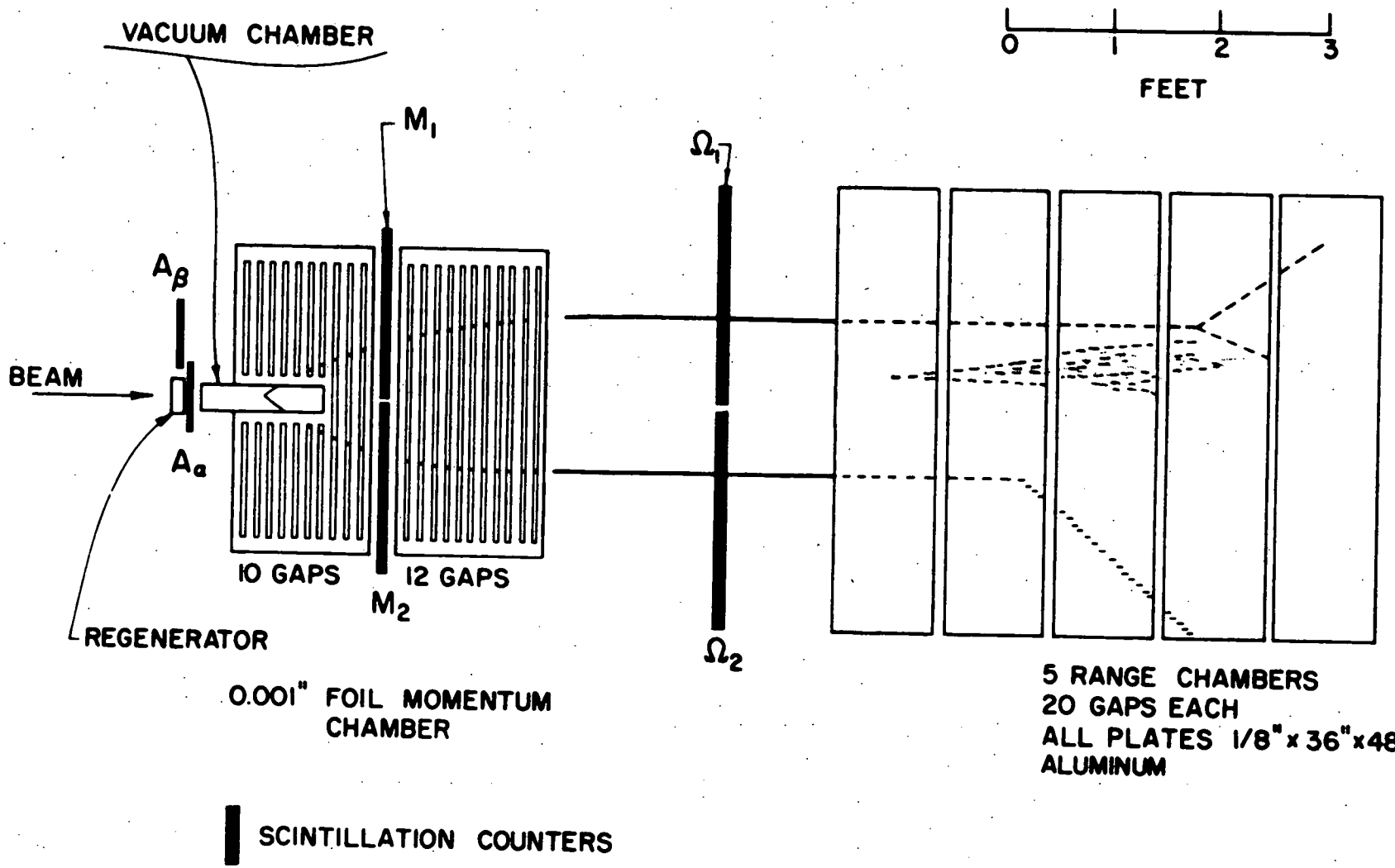

kilogauss over the region of interest. The pole faces were 30" long (beam direction) by 45" wide with the upper pole face being slotted in order to photograph the chambers from above. (See Fig. 5) The magnetic field polarity was reversed every seven rolls of film. The magnet was cycled during the polarity changes to eliminate hysteresis effects. In addition the current through the magnet and the voltage of a Hall probe inside the magnet were recorded for every roll of film.

The spark chambers were offset 6 inches to the right of the magnet centerline to make room for the side view mirrors. The chambers were securely attached to a large aluminum transport plate which rolled in and out of the magnet to enable us to service the chambers. When in the magnet, the transport plate was securely clamped in place. This was important not only to be sure that the chambers did not accidently change position during the run, but also to protect the chambers in case of a power failure. In the event of sudden field collapse the large eddy currents induced in the chambers and in the transport plate were capable of making the chambers and plate jump.

About 40" downstream from the second magnet chamber were five "range" or "shower" spark chambers made of 1/8" aluminum plates 36" high by 48" wide. There were twenty 5/16" gaps per chamber. Including the walls a particle passing through one chamber must traverse 7.62 cm of aluminum or .86 radiation lengths. Between the vacuum pipe and the first active gap of the shower

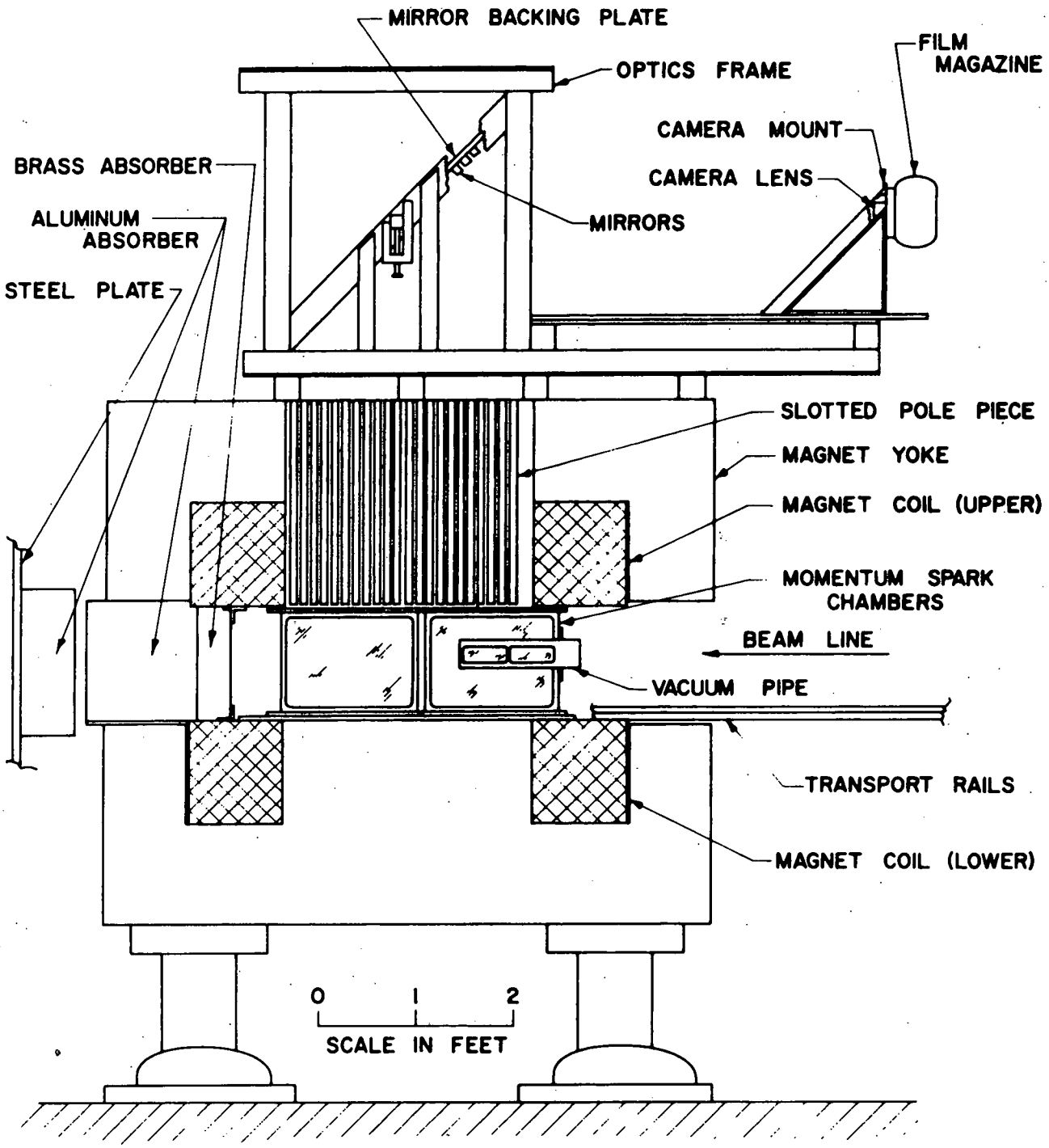

Figure 5. SPARK CHAMBERS AND MAGNET ELEVATION

chambers there were 4.3 gm/cm^2 of Al, 0.7 gm/cm^2 of Cu (radiation shield) and 1.9 gm/cm^2 of CH (plastic scintillator) for a total of 5.9 gm/cm^2 in all.

Both magnet and range spark chambers were filled with a 90% neon - 10% helium mixture at essentially atmospheric pressure. (Actually an overpressure of about 1/8" of silicone oil was maintained at all times.) The chamber gas was circulated through zeolite cold traps at liquid nitrogen temperatures to maintain the purity of the gas.

Six scintillation counters were involved in triggering the spark chambers. (See fig. 4 for the location of the counters.) Two of these, A_α and A_β were in anti-coincidence. A_α was immediately in front of the vacuum pipe. A_β was just to one side of the vacuum pipe to shield against stray charged particles. The anti-counters and the M_1 and M_2 counters were of 1/8" plastic scintillator and had long lucite light pipes to permit the photo-multiplier tubes to be in a region of low magnetic field. M_1 and M_2 were separated by 1/2" to reduce accidental coincidences in which a secondary particle from a neutron interaction in one counter would trigger the other. Ω_1 and Ω_2 which determined the solid angle of the secondary particles were 15" x 15" x 3/8" scintillators. Coincidence was demanded of counters M_1, M_2, Ω_1 and Ω_2. The triggering mode was intended to ensure that midway through the magnet the event had two charged particles which would reach the first plates of the range chambers.

University of Illinois Modular Electronics[29] was used. A block diagram of the electronic for the counter logic is shown in Fig. 6. For a detailed discussion of the spark chamber firing electronics and spark gaps see L. Verhey's thesis.[30]

The reproducibility of the counters was checked once a day when the beam was off. Standard counting rates for each counter were taken with and without a Co^{60} source. During the course of the run as photomultiplier tubes changed, the high voltage on each tube was adjusted to maintain the standard counting rate.

Four cameras with Beattie Coleman 35 millimeter film magazines and Schneider Super-Angulon lenses were used to photograph the spark chambers. To ensure correct correlation of film from different cameras, four octal counters which consisted of a total of 20 pairs of lights in blocks of three were photographed by each camera. The counters for all cameras were wired in parallel.

The top and the side view of the magnet chambers were recorded by the same camera. (See Fig. 5.) Each gap in the chambers was reflected in its own mirror strip atop the magnet and viewed through its own slot in the upper magnet pole face. A mirror on the side of each magnet chamber reflected the side view of each gap to the mirror strips above and thence to the camera. An event in the magnet chambers as it appeared on the film is shown in Fig. 7. A more detailed description of the magnet optics system can be found in Appendix B of R. J. Abram's Thesis.[31] Two top

Figure 6. DIAGRAM OF COUNTER LOGIC
USING "U of I" MODULAR ELECTRONICS

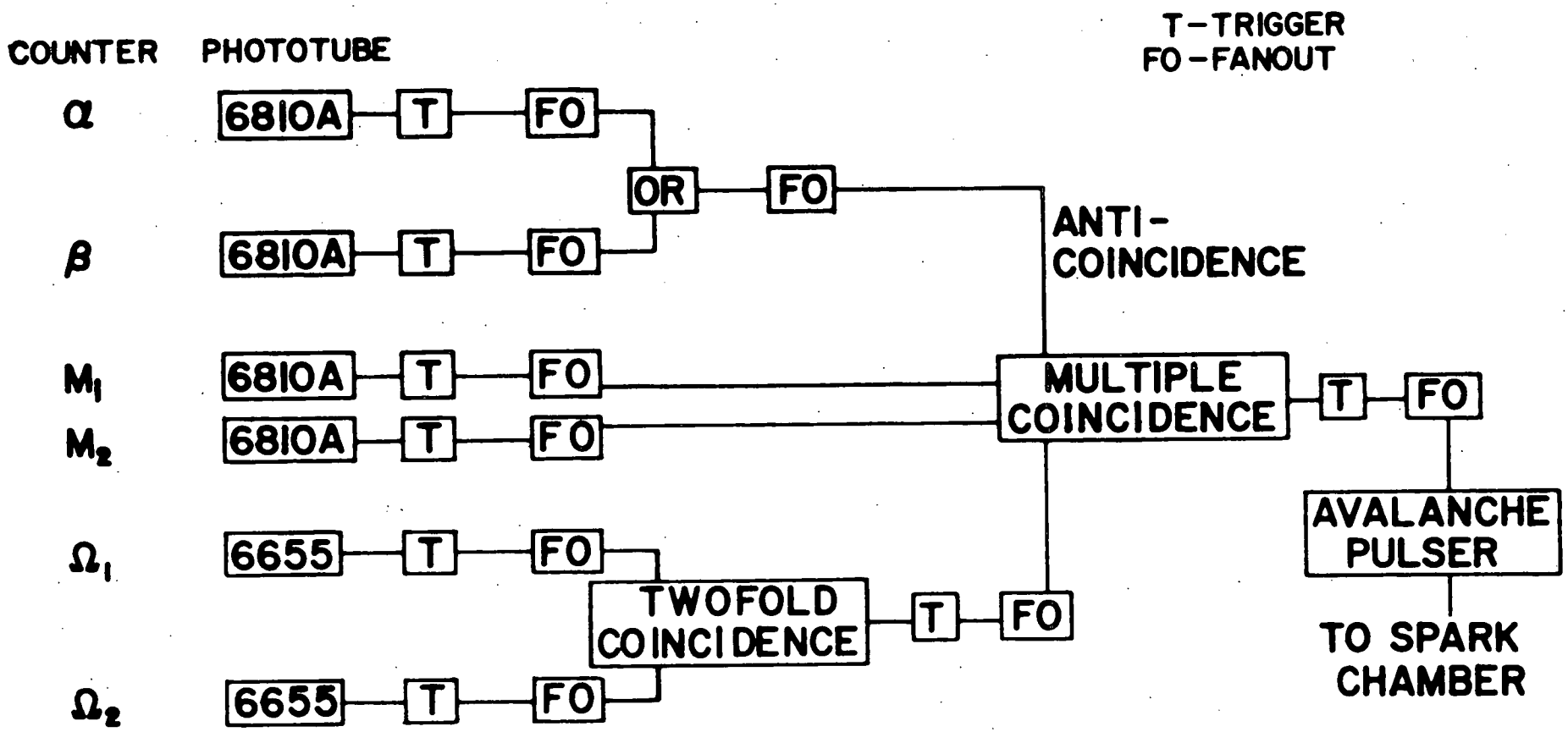

Figure 7. A typical event in the magnet chambers.

Figure 7. MAGNET CHAMBERS

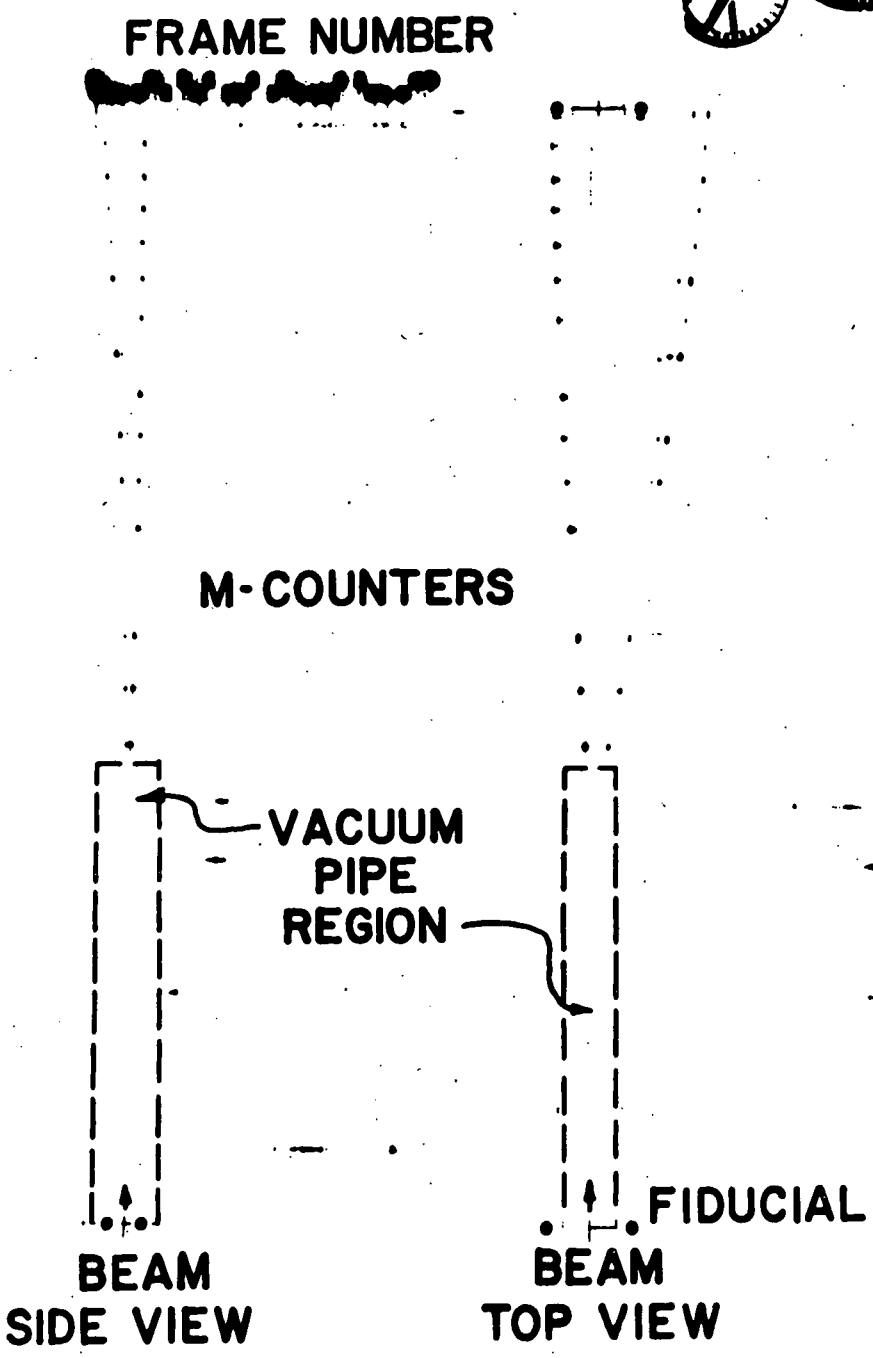

view cameras for the range or shower chambers were lined up with the outermost fiducial lines of the chambers to the left and right of the beam line. The top cameras in combination with the side camera at beam height gave both 80° and 100° stereo. An event in the range-shower chambers is shown in Fig. 8.

The cameras and the fiducial lines were set with the aid of the ANL survey group to an accuracy of better than 0.030" relative to the beam line. During the entire experiment a large survey monument was left in place over the beam line behind the apparatus.

A 1/2" thick piece of copper regenerator was position just upstream of the vacuum pipe during part of the run. See Fig. 4. The possible effects of this regenerator in our experiment will be discussed in Chapter V.

Figure 8. A typical event in the range-shower chambers.

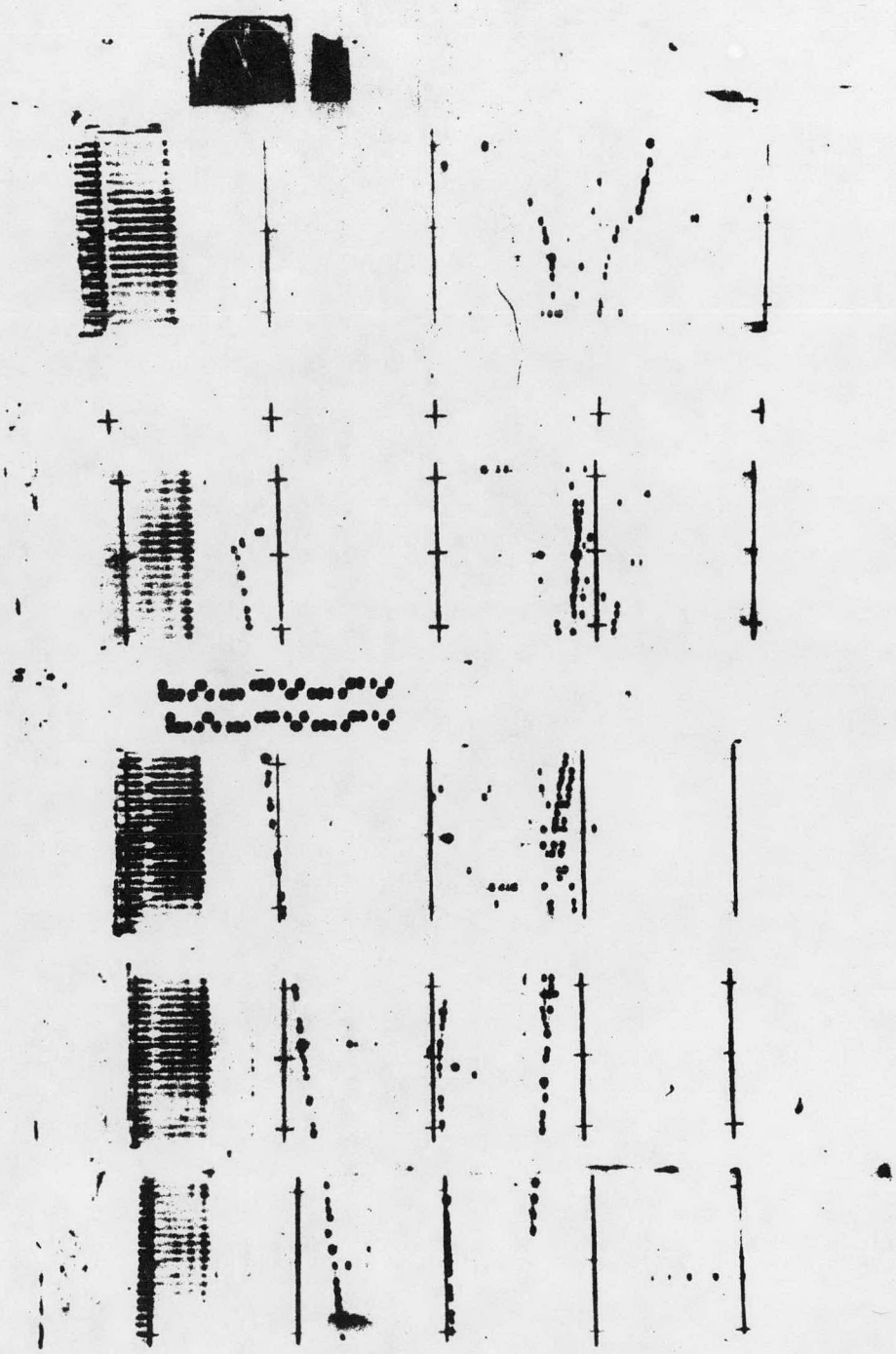

IV. REDUCTION OF DATA AND ANALYSIS

The film from the magnet chambers was scanned for events with good V's originating in the vacuum pipe with no extra tracks. The selected events were measured on CHLOE,[32] the Argonne National Laboratory's flying spot digitizer which was developed by D. Hodges and associates. The size and position of the sparks on the film were recorded by CHLOE on magnetic tape. The processing of events from this point on was done on the IBM 7094 computer at the University of Illinois. The pattern recognition programs (LINK) developed by R. Clark of the Argonne National Laboratory[33] were modified to handle more rapidly our particular set of event topologies by R. Mischke and O. McBride. If this streamlined set of programs failed to handle an event, then LINK was called. (See Mischke's thesis[34] for details.) A preliminary reconstruction and kinematic analysis was performed at this point and event summary cards were punched containing among other things the location of the spark in each track. Using these cards, we were able to incorporate later corrections for the non-uniformity of the magnetic field and also improved optical constants without doing pattern recognition over again.

A scan of the range-shower chamber film was made looking for gamma rays. Every frame was scanned regardless of the analysis of the magnet chamber film for the event. The scanners were given the following range-shower chamber scan rules.

1. Record all events for which there is a good gamma ray shower.
2. A good gamma ray shower must
   a) skip at least the first three gaps of chamber one (Otherwise it may be an electron shower.)
   b) point back toward the vacuum pipe region
   c) NOT point back to a track
   d) NOT originate in the beam as indicated on the beam templates.

   In general the opening angles of the electron-positron pair in a gamma ray shower is small. The higher the energy of the gamma ray, the smaller the opening angle.
3. To be labeled a pion, a track must do one of three things
   a) stop in the chamber. (Be careful not to be fooled by tracks going out the top, bottom or sides of the chamber.)
   b) interact in the chamber producing 2 or more prongs
   c) scatter through an angle of more than 5°.
4. For each good event, record the chamber and gap number of the gamma ray origin.
5. If a good event has 2 pions, then for each pion record
   a) the number of prongs
   b) the chamber and gap where the track stopped, kinked or interacted

c) the angles of scatter in the left and side views (for those pions which scatter or " kink").

6. If in doubt about an event, ask a physicist. If a physicist is not available, record the event. A lost event may never be found.

The scanners took rather seriously the admonition not to throw away events which were doubtful. Most of the questionable events were thrown out when checked by a physicist. (See below in the discussion of the fate of events.)

A prior scan of the shower chamber film had been made looking for the decay of K_L^o into $\pi^+\pi^-\pi^o$. The only difference in the scanning rules was that events in which two charged pions were identified in the range-shower chambers were recorded even though no gamma ray was found. The events found in this scan represented a kinematically selected group since only those events were looked at in the range-shower chambers which were compatible with $K_L^o \rightarrow \pi^+\pi^-\pi^o$ kinematics as determined from the momentum measurements in the magnet chambers. An event compatible with $K_{\pi 3}$ kinematics is always also compatible with $K_{\pi\pi\gamma}$ but not vice-versa. A comparison of this "3π scan" with the "gamma scan" gives a check on the scanning efficiency. The efficiency is discussed later in this chapter.

The summary cards for all events in which a gamma ray was recorded in either the 3π scan or the gamma scan were run through

two programs which incorporated all optical and magnetic field corrections. The first of these programs computed all relevent kinematic quantities for the decay under the hypotheses of K_{e3}, $K_{\mu 3}$, $K_{\pi\pi\gamma}$, and $K_{\pi 3}$ for both solutions for the energy of the kaon. In particular it calculated the direction cosines of the photon assuming the decay to be $K_L^o \rightarrow \pi^+ + \pi^- + \gamma$, so that one could predict the line of flight of the photon through the range-shower chambers. The two-fold ambiguity in the energy of the kaon presents no difficulty in this experiment. In general the two solutions arise because one does not know whether the neutral particle went forward or backward in the rest frame of the kaon. In the decay $K_L^o \rightarrow \pi^+\pi^-\gamma$, those photons going backward in the kaon rest frame either miss the shower chambers entirely or have too low an energy to produce the observed shower. Thus one need only consider the solution with the higher energy for the kaon.

The second program with which the summary cards were run traced the two charged particles through the magnetic field and predicted their entry points in the range-shower chambers. This program also checked whether the charged particles struck the magnet yoke where interactions with the iron could give rise to spurious gamma rays and also to charged secondaries which could falsely trigger the Ω (solid angle) counters.

With the output of these two programs at hand, a physicist looked at the shower chamber film for every event in which a gamma

shower had been reported. Using a special graph, he could quickly estimate the coordinates of a shower origin or of a charged particle track to about one inch.

It was then easy to screen out those K_{e3} events in which the electron had failed to produce sparks in the first three gaps of the chamber and had subsequently showered. The charged particle tracing program also facilitated the screening out of those events in which the shower came from a gamma ray produced in interactions with the back magnet chamber wall, the front shower chamber wall or the solid angle counters.

The events remaining after these checks should be almost entirely $K_{\pi 3}$ or $K_{\pi\pi\gamma}$ events. At this stage a comparison of the two scans becomes a significant measure of the scanning efficiency. Since the "3π scan" involved a preselection of events to look at whereas the "gamma scan" did not, the expression chosen as a measure of the scanning efficiency for gamma rays is

$$e_\gamma = 1 - \frac{\text{the number of good events found in the "}3\pi\text{ scan" but missed in the "gamma scan"}}{\text{the number of good events found in both scans}}$$

where for this purpose "good event" implies also that the event was kinematically compatible with $K_{3\pi}$ decay. As defined the scanning efficiency was found to be $e_\gamma = 87\%$.

Each event in which a gamma ray was reported was tested for compatibility with the hypothesis of $K_L^o \rightarrow \pi^+\pi^-\gamma$. The actual

position of the shower origin was compared with that predicted from the direction cosines of the photon which were computed in the program described above. All events in which the miss between the predicted and observed shower origin positions was less than 5 inches were remeasured to determine the actual shower origin with greater accuracy. About 1/3 of these were remeasured twice, first with left and side views and then with right and side views. The two measurements agreed always to better than 0.5 inches.

The "rate" of events is described below.

1. There were 160,000 pictures taken during the runs with 0" and 1/2" generator.

2. 71,000 of these pictures were found by scanners to have a "good V" in the momentum chambers suitable for digitization on CHLOE.

3. 92.4% of these or 66,000 were properly digitized. 6% should not have been on the scan list. Only 1.6% were lost because of poor digitization.

4. The pattern recognition programs failed on about 10% of the events which had been digitized. This left 59,500 events in the sample.

5. After cutoffs were imposed on the allowed region of decay 41,000 events remained.

6. From this sample, the scan of the shower chambers yielded 3,507 candidates.

position of the shower origin was compared with that predicted from the direction cosines of the photon which were computed in the program described above. All events in which the miss between the predicted and observed shower origin positions was less than 5 inches were remeasured to determine the actual shower origin with greater accuracy. About 1/3 of these were remeasured twice, first with left and side views and then with right and side views. The two measurements agreed always to better than 0.5 inches.

The "fate" of events is described below.

1. There were 160,000 pictures taken during the runs with 0" and 1/2" generator.

2. 71,000 of these pictures were found by scanners to have a "good V" in the momentum chambers suitable for digitization on CHLOE.

3. 92.4% of these or 66,000 were properly digitized. 6% should not have been on the scan list. Only 1.6% were lost because of poor digitization.

4. The pattern recognition programs failed on about 10% of the events which had been digitized. This left 59,500 events in the sample.

5. After cutoffs were imposed on the allowed region of decay 41,000 events remained.

6. From this sample, the scan of the shower chambers yielded 3,507 candidates.

7. After the test for kinematic compatibility with the $K \rightarrow \pi\pi\gamma$ hypothesis and the test to eliminate events in which one of the charged particles hit the magnet, 1570 candidates remained.

8. 962 of these candidates passed the scrutiny of the physicist. Most of the events thrown out at this point failed because the gamma shower was associated with one of the charged particles entering the chamber. Pion exchange with subsequent $\pi^{o} \rightarrow \gamma\gamma$ decay was the biggest contributor.

350 of the candidates were from the no regenerator run and 612 from the 1/2" regenerator run.

Three closely related Monte Carlo calculations were made on the IBM 7094 computer. Two of these involved the generation of $K_{\pi\pi\gamma}$ events, in the first place to calculate the detection efficiency for this decay and in the second to determine the effect of measurement error on the predicted photon trajectory and shower origin. The third Monte-Carlo program was to determine the $K_{\pi 3}$ detection efficiency since it is the $K_{\pi 3}$ rate to which we wish to normalize our measurement of the $K_{\pi\pi\gamma}$ rate.

The $K_{\pi\pi\gamma}$ detection efficiency program was the simplest of the three. In it the events were generated in the center of mass system according to a uniformly populated Dalitz plot. The justification for assuming a uniformly populated Dalitz plot is that none of the various calculations for the energy spectrum of the photon differs very much from phase space. Furthermore by

recording the center of mass energy of the photon for the successful Monte Carlo events one can determine the detection efficiency for different regions of the Dalitz plot. If one were to detect a reasonable number of $K_L^o \to \pi^+\pi^-\gamma$ events, then one could infer something about the decay interaction.

The energy of the K-meson was picked randomly according to the observed beam spectrum. The momenta of the decay products were transformed to the laboratory system. At this stage a decay point was picked randomly from the acceptable region and the paths of the two charged particles were traced through the non-uniform magnetic field.

Tests were made to check that all the required counters were triggered and that the charged particles did not hit the magnet yoke. If the event was a "good trigger", the laboratory energy of the photon was required to be greater than some minimum value. (See below.) Then the trajectory of the photon was checked to see that it would pass through at least two interaction lengths in the shower chambers. If the event passed this test, it was taken as a "success" and the relevant parameters of the decay were recorded.

For the $K_{\pi 3}$ detection efficiency the program differed in two respects. First, the events in the center of mass system were generated according to a Dalitz plot which incorporated the matrix element dependence of the population density.[35] The expression used is:

$$\text{Density} \propto 1 + \frac{2M_K \sigma}{m_\pi^2} (2T_3 - T_{max})$$

where T_3 is the kinetic energy of the π_o

T_{max} is the maximum kinetic energy of the π^o

m_k is the mass of the K

m is the mass of the π

and σ is an experimentally determined parameter[35] taken to be $= -0.21$.

The other difference is that for $K_{3\pi}$, the π^o must be allowed to decay in a random plane and the laboratory energy and trajectory of both the resultant photons must be checked.

The efficiency found for either decay mode depends on the minimum photon energy required. (See Fig. 9 for graphs of $\varepsilon_{\pi\pi\gamma}$, $\varepsilon_{\pi 3}$ and $\varepsilon_{\pi 3}/\varepsilon_{\pi\pi\gamma}$ versus the cutoff of the gamma ray laboratory energy. We estimate that the right cutoff is 250 $\pm$ 50 MeV. This corresponds to a detection efficiency for $K_{3\pi}$ or $\varepsilon_{\pi 3} = (1.31 \,^{+.21}_{-.24}) \times 10^{-2}$ and for $K_{\pi\pi\gamma}$ of $\varepsilon_{\pi\pi\gamma} = (1.12 \,^{+.11}_{-.12}) \times 10^{-2}$. The ratio is then $\varepsilon_{\pi 3}/\varepsilon_{\pi\pi\gamma} = 1.17 \,^{+.05}_{-.04}$.

The remaining Monte Carlo program was to determine the effect on the predicted shower origin of measurement errors in the spark locations. $K_{\pi\pi\gamma}$ events were generated exactly as in the $K_{\pi\pi\gamma}$ detection efficiency program. "Spark locations" were assigned to the intersection of each charged particle (pion) trajectory as determined by the ray tracing program. These "sparks" were then

Figure 9. Detection efficiencies for the decay modes $K_L^o \rightarrow \pi^+\pi^-\gamma$ and $K_L^o \rightarrow \pi^+\pi^-\pi^o$ versus the cutoff in the laboratory energy of the gamma ray.

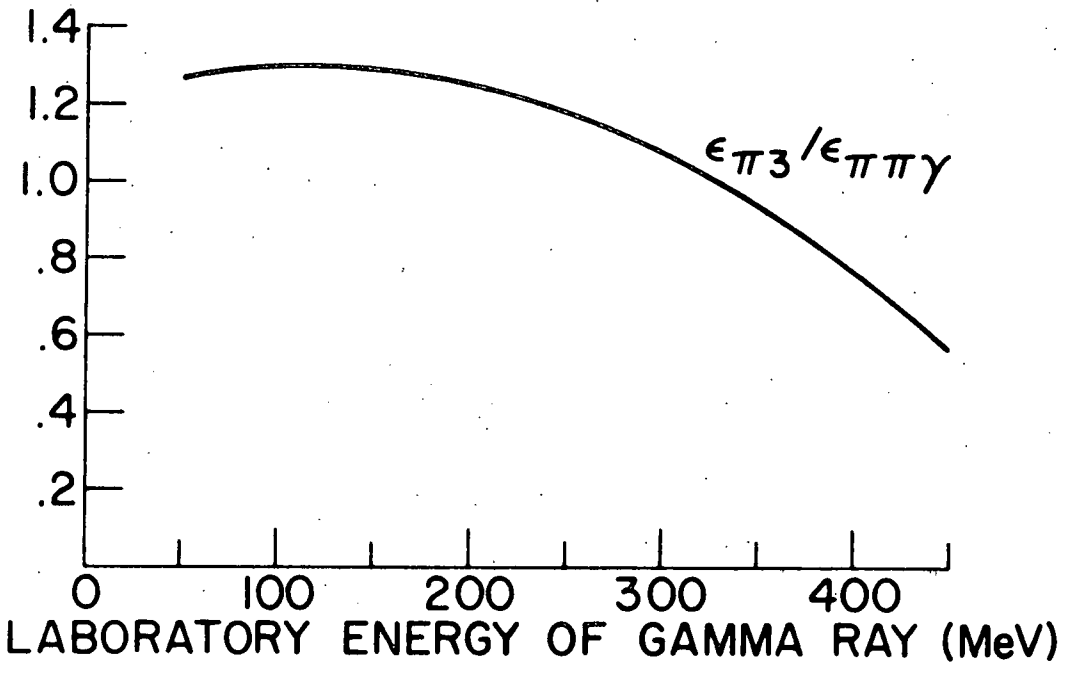
1.4
1.2
1.0
.8
.6
.4
.2
$\epsilon_{\pi 3}/\epsilon_{\pi\pi\gamma}$
0
100
200
300
400
LABORATORY ENERGY OF GAMMA RAY (MeV)

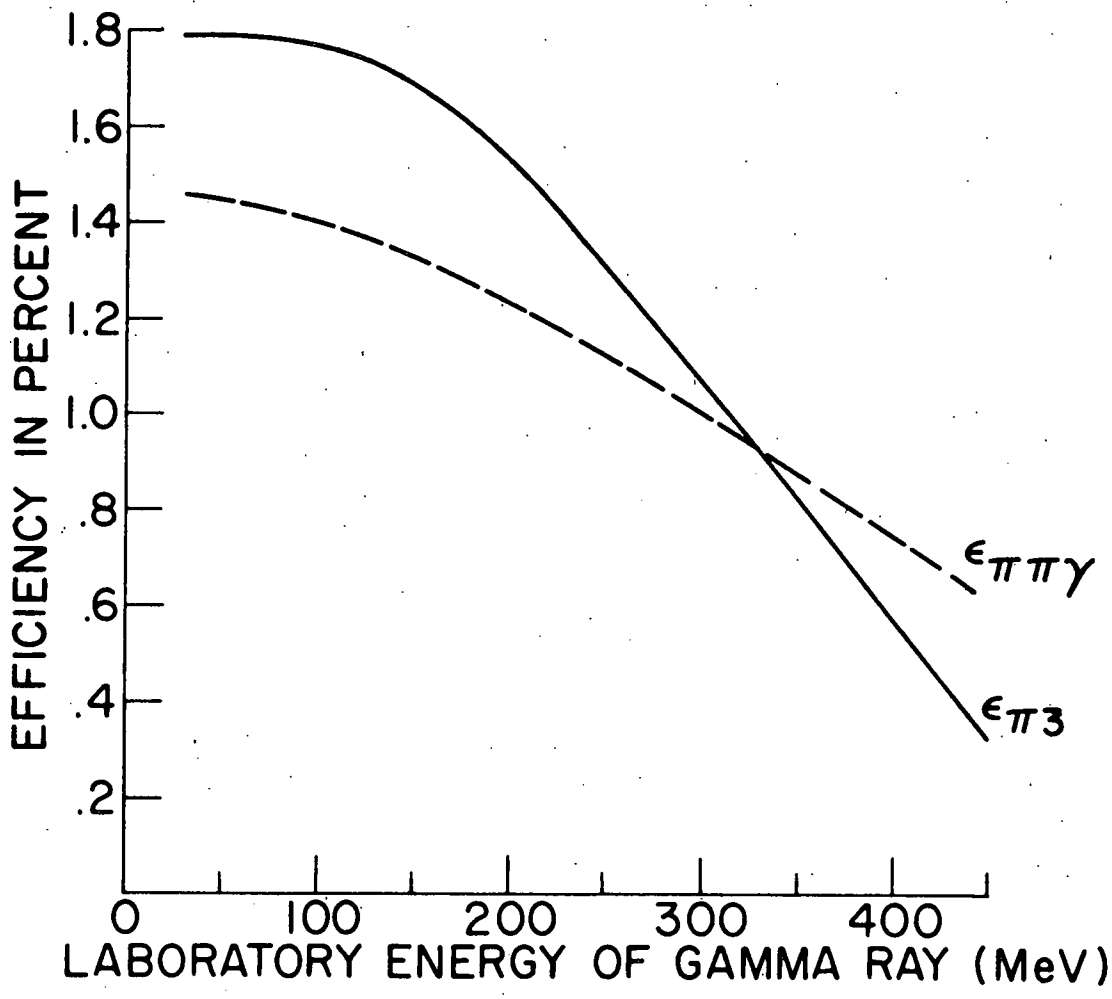
1.8
1.6
1.4
1.2
1.0
.8
.6
.4
.2
EFFICIENCY IN PERCENT
$\epsilon_{\pi\pi\gamma}$
$\epsilon_{\pi 3}$
0
100
200
300
400
LABORATORY ENERGY OF GAMMA RAY (MeV)

shifted randomly with Gaussian-distributed measurement "errors". From the new spark positions the Monte-Carlo event was reconstructed in the same way as for an actual event and the entry point of the photon in the shower chambers was calculated. The comparison of the computed entry positions before and after the introduction of "measuring error" tells us how much uncertainty in this position is introduced in the measurement of the magnet chamber sparks. This calculation hinges on the width of the Gaussian error distribution used. In the above calculations in order to be pessimistic, the r.m.s. value for the error distribution was chosen to be 0.020" both vertically and horizontally. In the course of processing many events on this film for this and other experiments the r.m.s. deviation from a fitted helix in the vertical was 0.018" and in the horizontal was 0.012". Therefore the value 0.020" is compatible with the CHLOE least count of 0.016" and allows for small uncorrected errors in the optics. With this value the r.m.s. "miss" between the computer entry positions before and after "measuring error" was 0.47".

V. RESULTS AND DISCUSSION

One way of displaying the experimental results is in the form of a histogram of the number of events having various values of "miss" for the photon that is shown in Fig. 10. The "miss" plotted is the distance in real space between the actual origin and the predicted origin of the gamma ray shower. The "miss" $\Delta R = \sqrt{\Delta X^2 + \Delta Y^2}$ where ΔX is the difference in the X coordinates between the observed and predicted shower origins and similarly for ΔY. (X and Y are transverse to the beam.)

One expects that gamma ray showers arising from the 3π decay mode of the K_L^o meson will be virtually the sole background and that these should be distributed essentially uniformly in X and Y throughout the shower chambers. The assumption of uniform distribution of background is supported by the plot in Fig. 11 showing the X and Y coordinates of about 100 gamma ray showers observed.

Under the assumption of uniform background the data in Fig. 10 were fitted by the least squares method to a straight line passing through the origin. The resulting line has a slope of 4.25. The X^2 of this fit is 6.53 for 7 degrees of freedom. We note that there is no indication of any peaking above the background near the origin. With our resolution any real event should be in the first bin.

Figure 10. Histogram of the "miss" between expected and actual shower-origin positions. The straight line fitted to the data has a chi-square value of 6.53.

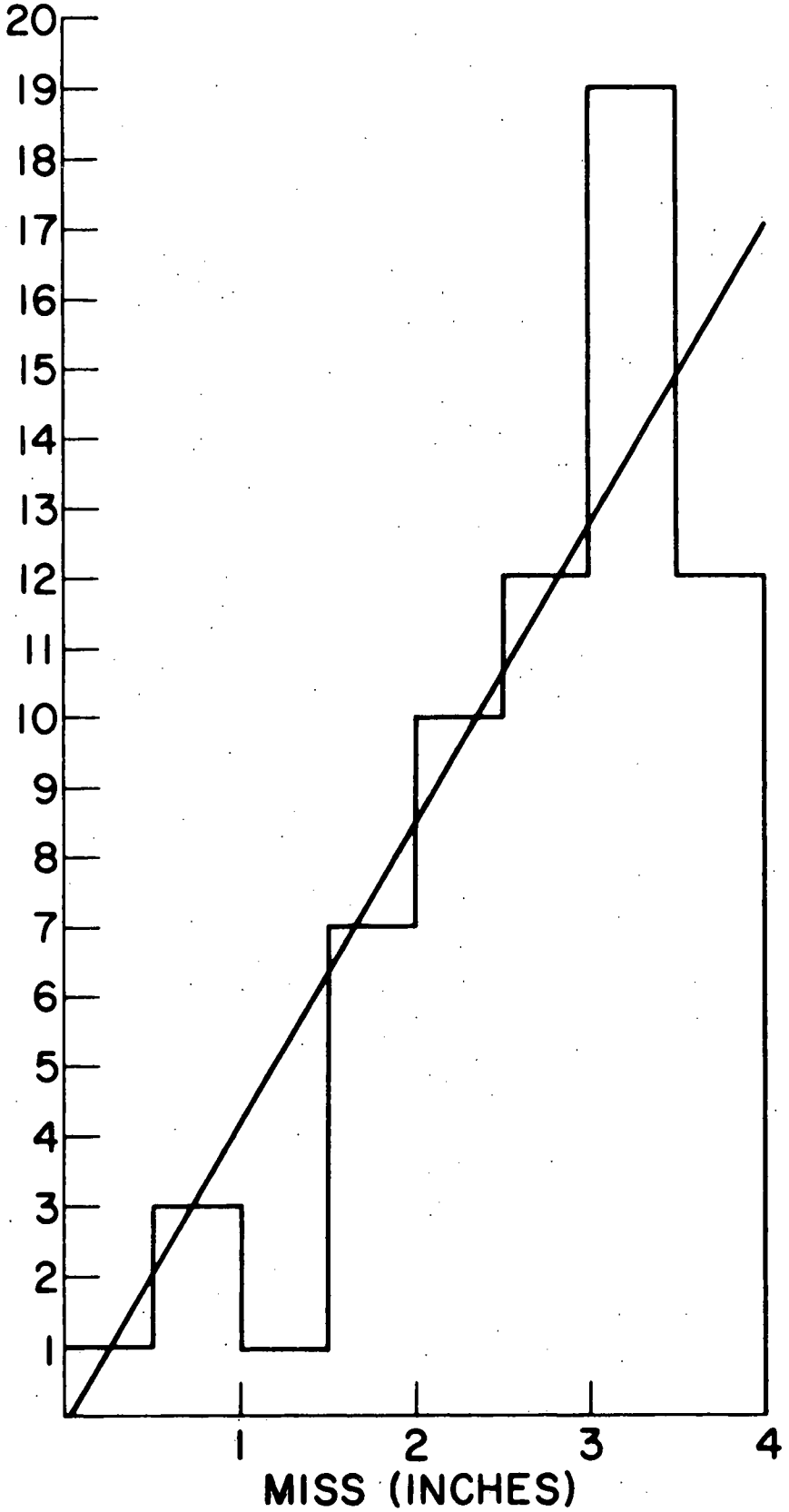
20
19
18
17
16
15
14
13
12
11
10
9
8
7
6
5
4
3
2
1
1
2
3
4
MISS (INCHES)

Figure 11. The distribution of the gamma ray showers in the chambers.

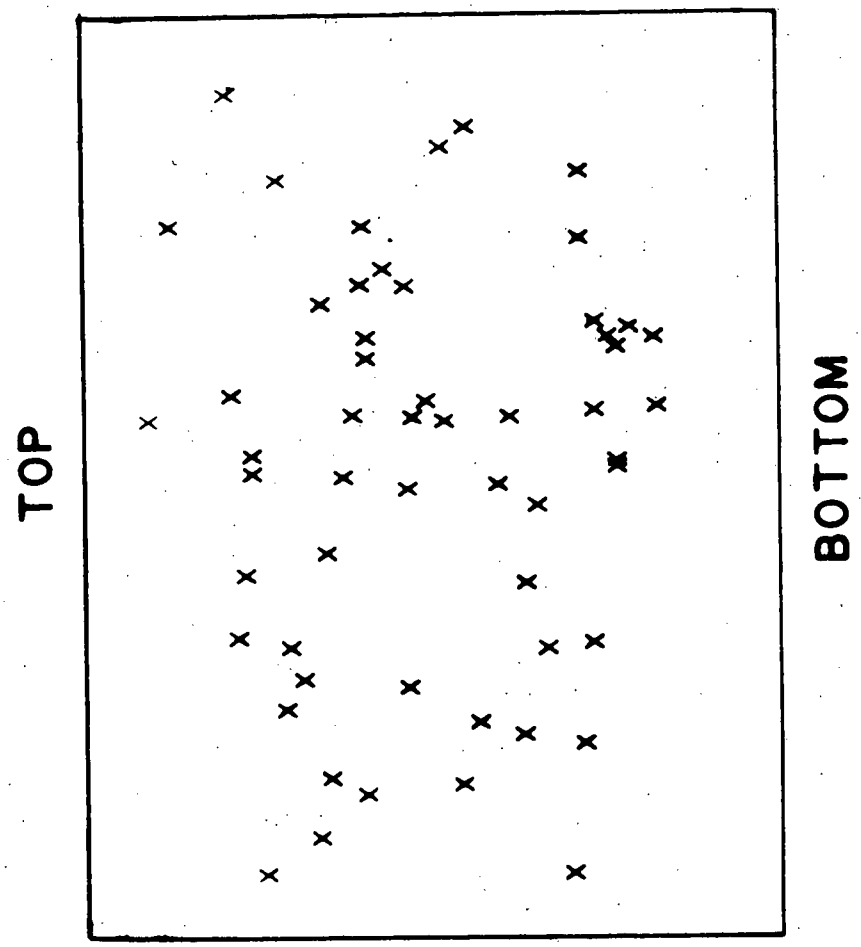
TOP
BOTTOM

An alternative way of displaying the experimental results is to plot where the individual γ-rays were observed relative to their expected position. This is shown in Fig. 12. It also allows us to check that there is no peak shifted in some systematic way from the origin. The plot was made of the X and Y components of the "shower origin miss" (+X up, +Y to the right facing downstream) of each event with "miss" less than five inches. We see that there is no peak. The most one can say about the plot is that if one shifted the ΔX axis down by about 0.4" ($\Delta Y = \Delta Y + 0.4$), the distribution by quadrant of the events would be slightly more symmetric.

Population of Quadrants

	I	II	III	IV
Without shift	22	18	38	24
With 0.4" shift	24	24	32	22

However more important to note is that the change produced in the histogram of "miss" (Fig. 10) is completely negligible and does not produce a peak near the origin.

With or without a shift of 0.4" there is one and only one event with a "miss" smaller than our resolution. However, as one can see from the background fit, one background event is expected in the first bin. Since this is the case, the only thing we can do is to set an upper limit on the decay rate and evaluate the confidence level corresponding to this limit.

Figure 12. The distribution of shower-origin miss.

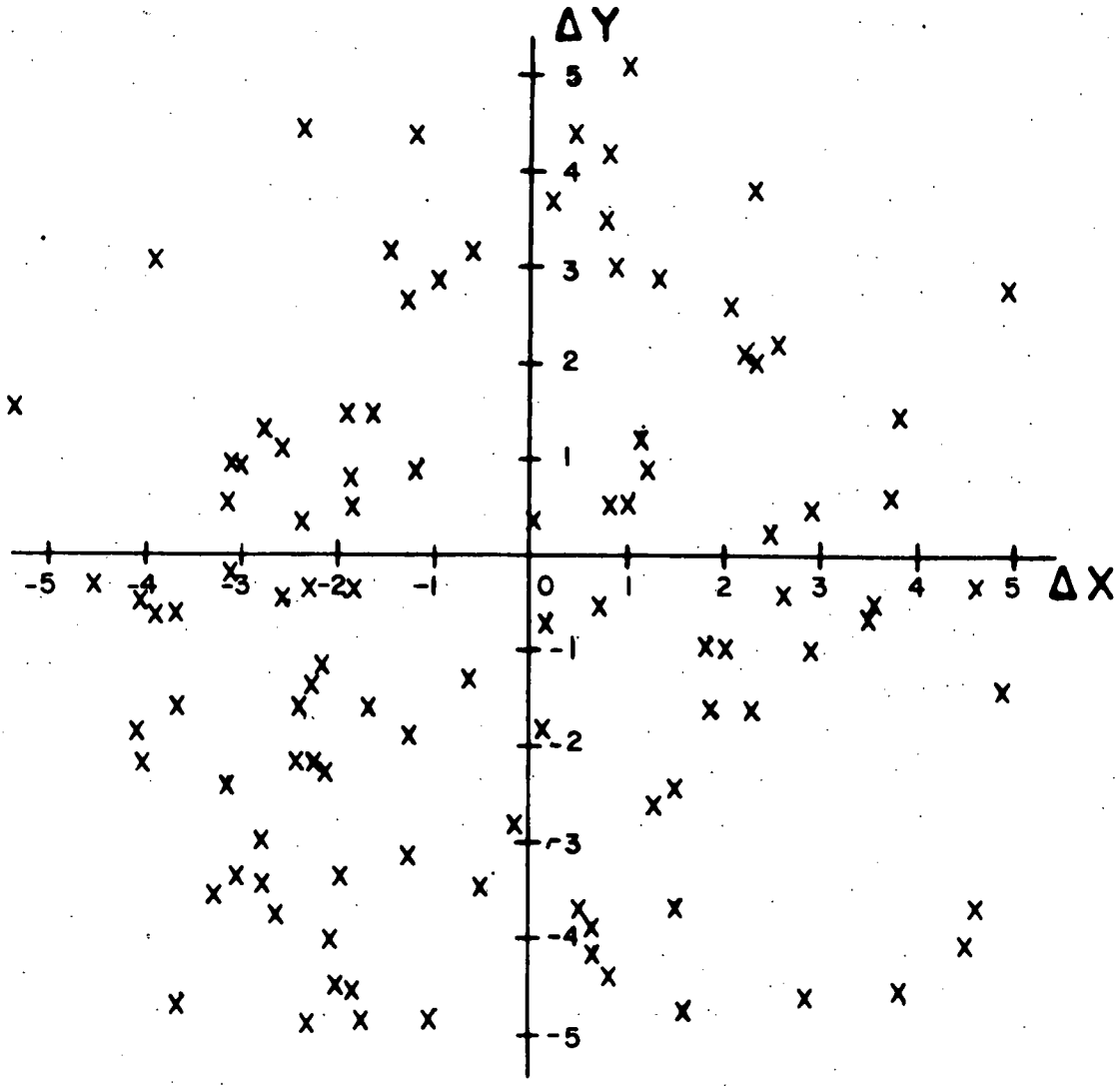
ΔY
ΔX
5
4
3
2
1
-1
-2
-3
-4
-5
-5
-4
-3
-2
-1
0
1
2
3
4
5

If we had found $N_{\pi\pi\gamma}$ events above background, then we would have determined the branching ratio to be

$$\frac{R(K_L^o \to \pi^+\pi^-\gamma)}{R(K_L^o \to \text{all})} = \frac{N_{\pi\pi\gamma}}{N_{\pi 3}} \times \frac{\varepsilon_{\pi\pi\gamma}}{\varepsilon_{\pi 3}} \times \frac{R(K_L^o \to \pi^+\pi^-\pi^o)}{R(K_L^o \to \text{all})} \qquad (20)$$

where $N_{\pi 3} = 962$, the number of $K_{\pi 3}$ events believed to be in the sample and $\frac{\varepsilon_{\pi 3}}{\varepsilon_{\pi\pi\gamma}} = 1.17$, the ratio of the detection efficiencies found in chapter IV. But we have no events above background so we report an upper limit on the branching ratio. That is we replace the = sign in Eq. (20) by $\leqslant$ and $N_{\pi\pi\gamma}$ is replaced by $N_{\pi\pi\gamma}(\text{max})$, the number of $\pi\pi\gamma$ events which would be expected in our data if the branching ratio really were to be our upper limit. The higher we choose $N_{\pi\pi\gamma}(\text{max})$ to be, the higher the upper limit we set and the more confidence we can have in this upper limit. Evaluating the probability (confidence level) that an upper limit is all right is rather involved so before discussing confidence levels we first state the upper limits corresponding to $N_{\pi\pi\gamma}(\text{max}) = 1,2,$ and 3 events in our data

$N_{\pi\pi\gamma}(\text{max})$	Upper limit on $R(K_L^o \to \pi^+\pi^-\gamma)/R(K_L^o \to \text{all})$
1	1.4×10^{-4}
2	2.8×10^{-4}
3	4.2×10^{-4}

One expects that both the number of real $K_{\pi\pi\gamma}$ events and the number of background events will follow Poisson distributions:

$$P(k,\mu) = \frac{\mu^k e^{-\mu}}{k!}$$

where k is the number of events observed in a given trial and μ is the mean number of events expected. In a situation such as ours in which an event can come from either of two random and indistinguishable processes, the distribution of events is given by a single Poisson distribution in which the mean is just the sum of the two individual distributions.

Thus the probability of observing k events, either real or background is

$$P(k;\ \mu_r,\ \mu_b) = \frac{(\mu_r + \mu_b)^k\ e^{-(\mu_r+\mu_b)}}{k!}$$

where

μ_r = mean of the distribution for real $K_{\pi\pi\gamma}$ events

μ_b = mean of distribution for background events.

From Fig. 10 we see that there is one event within our experimental resolution and that one event is expected from background. That is, k = 1 and μ_b = 1. Let us now find the

probability (confidence level) that the upper limit on the branching ratio corresponding to $N_{\pi\pi\gamma}(\max)$ events in our sample is really all right. This is just

$$\text{Confidence Level} = 1 - P(k = 1; \mu_r \geqslant N_{\pi\pi\gamma}(\max), \mu_b = 1)$$

where $P(k = 1, \mu_r \geqslant N_{\pi\pi\gamma}(\max), \mu_b = 1)$ is the probability of getting our result (one event) with the expectation value μ_r having any value $\mu_r \geqslant N_{\pi\pi\gamma}(\max)$.

$$\begin{aligned} & P(k = 1, \mu_r \geqslant N_{\pi\pi\gamma}(\max), \mu_b = 1) \\ &= \int_{N_{\pi\pi\gamma}}^{\infty} P(k = 1, \mu_r, \mu_b = 1)\, d\mu_r \\ &= \int_{N_{\pi\pi\gamma}(\max)}^{\infty} (1 + \mu_r)\, e^{-(\mu_r + 1)}\, d\mu_r \\ &= (N_{\pi\pi\gamma}(\max) + 2)\, e^{-(N_{\pi\pi\gamma}(\max) + 1)} \end{aligned} \tag{24}$$

This is the probability that $N_{\pi\pi\gamma}(\max)$ corresponds to too low an upper limit on the branching ratio. The confidence level is thus

$$\text{C.L. } (N_{\pi\pi\gamma}(\max))$$

$$= 1 - P(N_{\pi\pi\gamma}(\max) \text{ too low})$$

$$= 1 - (N_{\pi\pi\gamma}(\max) + 2)\, e^{-N_{\pi\pi\gamma}(\max)} - 1$$

$$\text{C.L. } (N_{\pi\pi\gamma}(\max) = 1) = 59.8\%$$

$$\text{C.L. } (N_{\pi\pi\gamma}(\max) = 2) = 80.4\%$$

$$\text{C.L. } (N_{\pi\pi\gamma}(\max) = 3) = 90.0\%$$

Our results may now be summarized.

Upper Limit on Rate	Upper Limit on Branching Ratio	Confidence Level
2.5×10^3 sec^{-1}	1.4×10^{-4}	59.8%
5.0×10^3 sec^{-1}	2.8×10^{-4}	80.4%
7.5×10^3 sec^{-1}	4.2×10^{-4}	90.0%

It is also relevent to note that all the events with a small "miss" in Fig. 10 were compatible with $K_{3\pi}$ decay. If a $K_{\pi 3}$ event is assumed to be $K_{\pi\pi\gamma}$, the predicted energy of the photon in the center of mass is always greater than 117 MeV. We found a handful of events with $E_\gamma < 117$ MeV but the "miss" was always greater than 3.5 inches.

Obviously, the value of the ratio of the efficiencies is important in obtaining the upper limit to the branching ratio. As a final check on our efficiency calculation, we have compared our findings with those for the K_{e3} data on the same film for the part of the run with no regenerator. From the number of K_{e3} events ($N_{K_{e3}}$) found in the sample, the branching ratios and the detection efficiencies $\varepsilon_{\pi 3}$ and ε_{e3}, one can estimate how many $K_{\pi 3}$ events one expects.

$$N_{\pi 3} = \text{Branching ratio } \left(\frac{K_{\pi 3}}{K_{e3}}\right) \times \frac{\varepsilon_{\pi 3}}{\varepsilon_{e3}} \times N_{K_{e3}}$$

In the no regenerator film, L. Verhey found 878 K_{e3} events and estimated the detection efficiency for this mode to be $\varepsilon_{e3} = 0.01$. Using these numbers plus those in the Rosenfeld table for branching ratios, we find

$$N_{\pi 3} = \frac{0.115}{.374} \times \frac{1.31 \times 10^{-2}}{1 \times 10^{-2}} \times 878 = 355 \text{ events}$$

This agrees very well with the 350 events which we found with good gamma-ray showers and this agreement gives us confidence in our

Monte Carlo efficiency program for $K_{\pi 3}$. Since this efficiency program is almost identical to that for $K_{\pi\pi\gamma}$, our confidence in the $\pi\pi\gamma$ program is also strengthened by the good showing of the 3π efficiency; however, the $\pi\pi\gamma$ efficiency does depend on the gamma ray spectrum in the center of mass.

For our $\pi\pi\gamma$ efficiency we chose to run with the spectrum corresponding to phase space. We will give further justification of that decision here. As remarked in Chapter IV, running the Monte Carlo program using phase space for the gamma ray spectrum gives us the efficiency as a function of the energy of the gamma ray in the center of mass. See Fig. 13 for a graph of this efficiency function. From this efficiency function we can then compute what the overall efficiency would be for any gamma ray spectrum we choose to consider. Lai and Young have calculated the gamma ray spectrum for their model for direct emission. Their spectrum and the phase space spectrum are shown in Fig. 14. Using our efficiency function and the spectrum of Lai and Young, we obtain an overall efficiency which is 5% smaller than that obtained from phase space. Thus we feel that reporting our upper limit on the $K_L^o \to \pi^+\pi^-\gamma$ rate on the basis of the phase space gamma spectrum is the best policy. Anyone with a different spectrum can then compute the corresponding overall efficiency using the efficiency function of Fig. 13. If their $\pi\pi\gamma$ detection efficiency is lower than the one obtained from phase space, then the upper limit of the $\pi\pi\gamma$ rate is raised proportionately.

Figure 13. The detection efficiency (in arbitrary units) for $K_L^o \rightarrow \pi^+\pi^-\gamma$ versus the energy of the gamma ray in the center of mass.

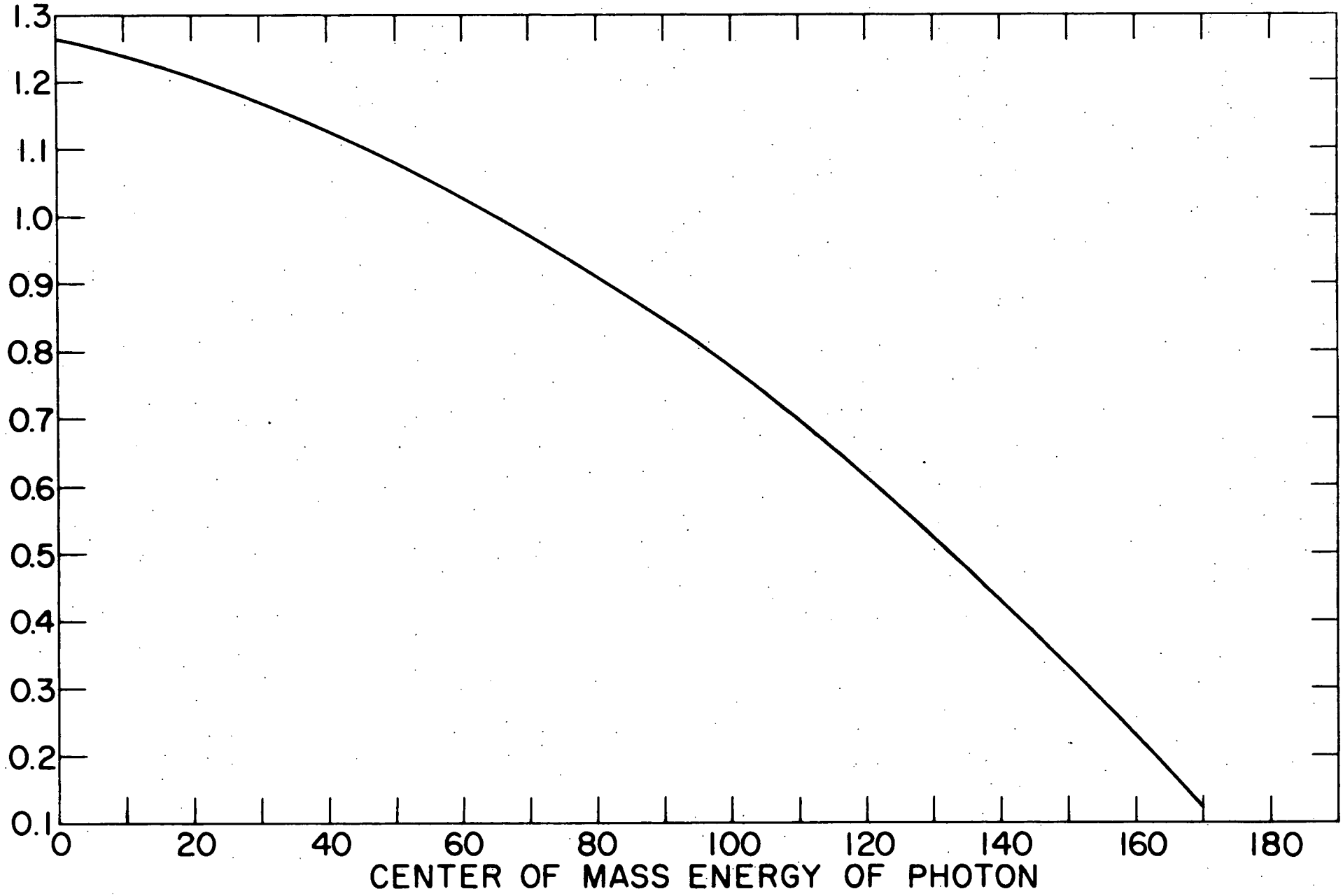
1.3
1.2
1.1
1.0
0.9
0.8
0.7
0.6
0.5
0.4
0.3
0.2
0.1
0
20
40
60
80
100
120
140
160
180
CENTER OF MASS ENERGY OF PHOTON

Figure 14. The center-of-mass energy spectrum for the gamma ray in $K_L^o \rightarrow \pi^+\pi^-\gamma$. The dashed line is phase space. The solid line is the spectrum in the theory of Lai and Young.

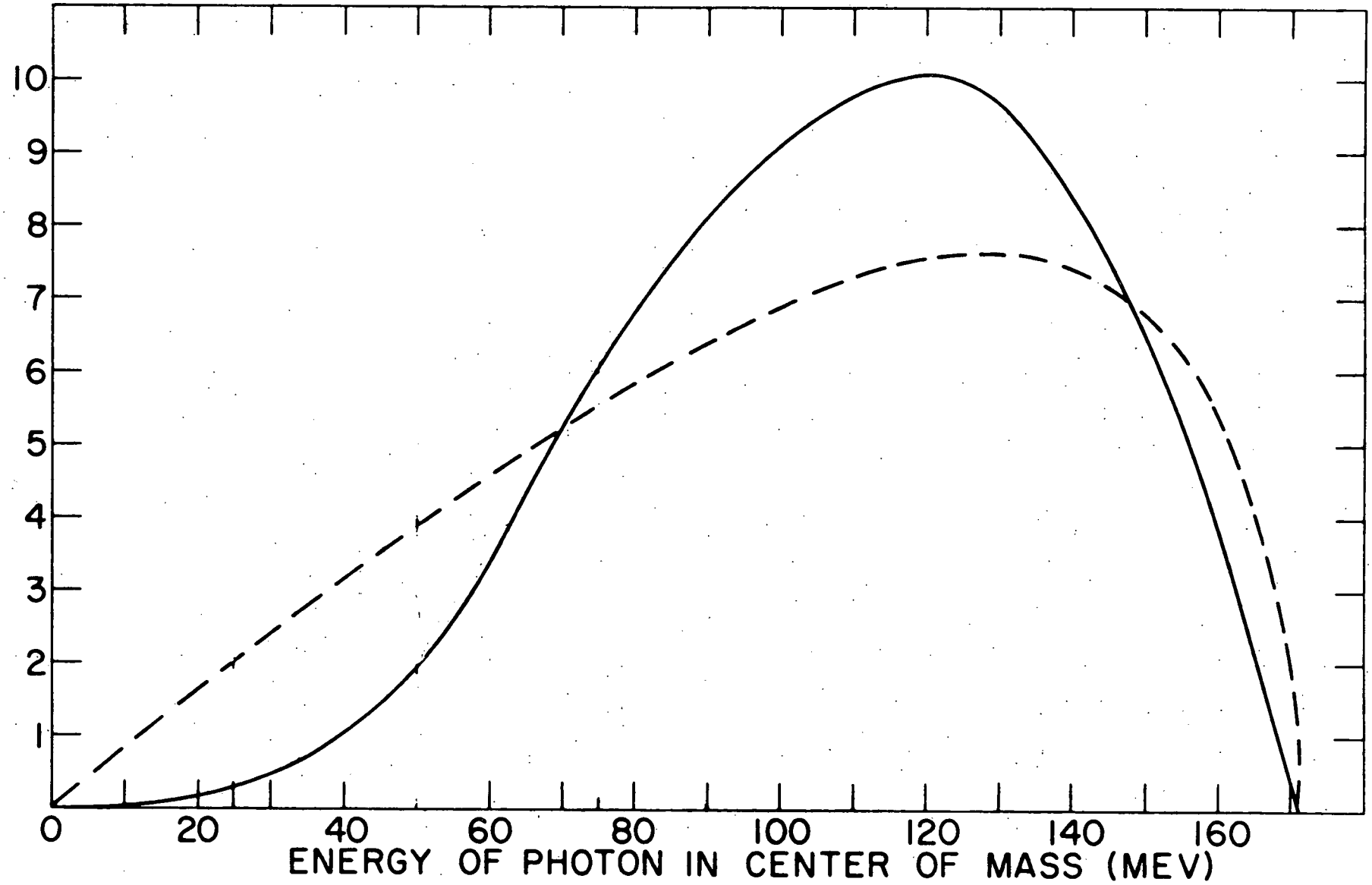
10
9
8
7
6
5
4
3
2
1
0
20
40
60
80
100
120
140
160
ENERGY OF PHOTON IN CENTER OF MASS (MEV)

In part of the run a 1/2" Cu regenerator was present. One needs to consider if there are any possible effects on the observed data due to this regenerator. The presence of the 1/2 inch copper regenerator in front of the vacuum pipe can have three effects. First, it could contribute $K_S^o \rightarrow \pi^+\pi^-\gamma$ events which we could not distinguish from $K_L^o \rightarrow \pi^+\pi^-\gamma$. Since in this experiment we found no events, this regeneration effect is of no concern to us. Secondly, gamma rays arising from bremsstrahlung in the copper are no problem since the charged particle involved would have to pass through the anti-counter. Thirdly, some of the K mesons scatter in the regenerator and then decay. For such events we will get wrong answers in the kinematics analysis. In particular, a $K_L^o \rightarrow \pi^+\pi^-\gamma$ event following such a scatter would result in a bad prediction for the gamma conversion point. Such events would be lost. If a $K_L^o \rightarrow \pi^+\pi^-\pi^o$ decay occurred after the K scattered in the copper, a fraction of these would appear kinematically incompatible with $K_{3\pi}$ and would not be used in the normalization. If one estimates the diffraction cross section to be 600 mb, one finds that less than 6.5% of the K's should undergo diffraction scattering in the regenerator. Looking at the number of events with good gamma showers one sees

No Regenerator	1/2" Regenerator
350 events	612 events
67 rolls of film	116 rolls of film
5.23 events/roll	5.29 events/roll

The number of events per roll is the same within statistics. Also the plots of the "miss" of the shower-origin are not statistically different. See Fig. 15. Therefore this effect does not give rise to a significant correction to our upper limit.

We would like to consider the significance of our result. We shall take the upper limit on the branching ratio to be 4.2×10^{-4} corresponding to a 90% confidence level. This is equivalent to an upper limit on the decay rate of 7.5×10^{3} sec^{-1} which is larger than all estimates of the rate except that of Pepper and Ueda. We see that their estimate (1.2×10^{4} sec^{-1}) is too high by about a factor of two. That Pepper and Ueda obtain such a large answer is interesting since Oneda, Kim, and Korff get 1/20 as big a rate when they compute the same diagrams plus some others. However, Pepper and Ueda have a very large destructive interference effect in their calculation so that their rate is the difference between two much larger rates. For this reason, their calculation is very sensitive to the choice of the coupling constants. Since Pepper and Ueda claim they only know the coupling constants to an order of magnitude, they can probably fix up their answer without resorting to any new mechanisms.

We must stress that our upper limit for $K_L^o \to \pi^+\pi^-\gamma$ is a full order of magnitude above the rate for inner bremsstrahlung alone. Therefore it is of interest to improve our measurement by a factor of at least five to test the other theoretical predictions of the direct process.

Figure 15. Histograms of the gamma ray shower-origin miss.

a) for the 1/2" regenerator data,

b) for the no regenerator data.

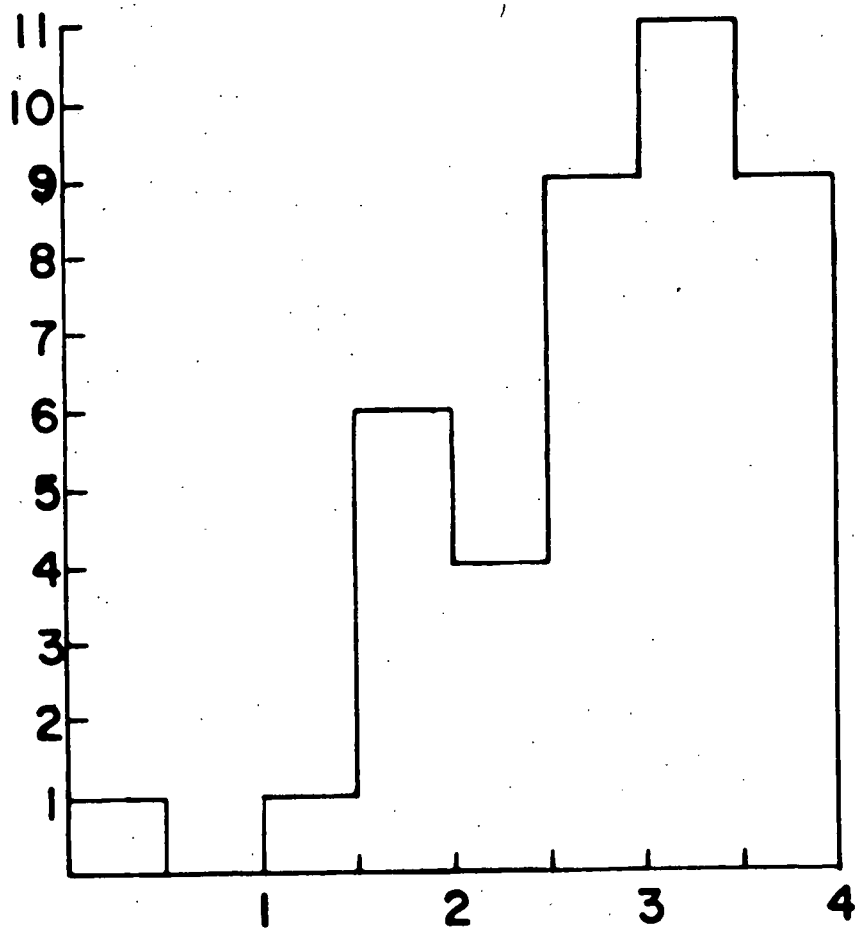

(a)

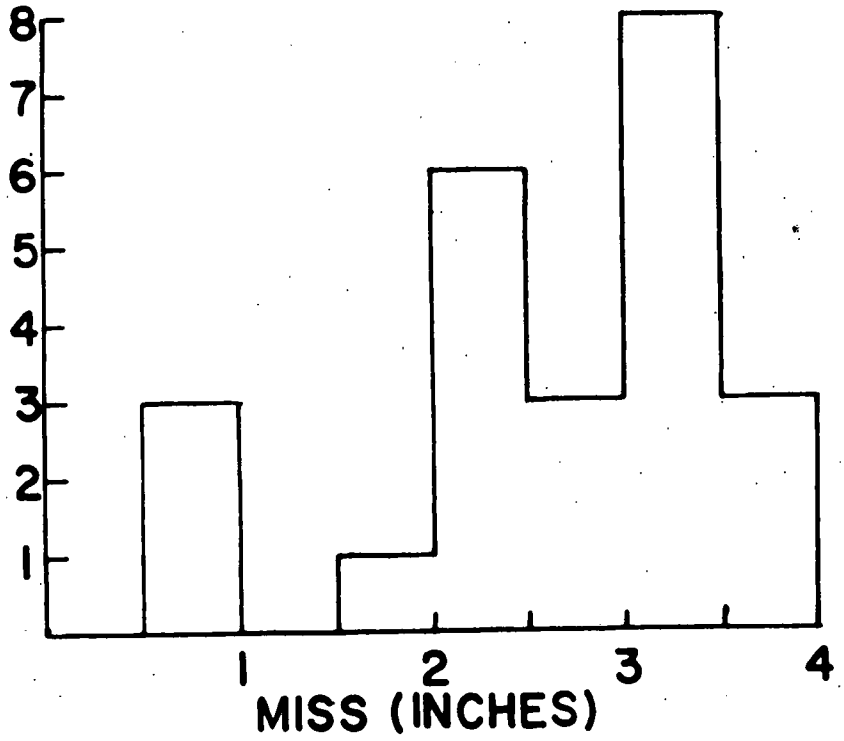

(b)

Is there a way to relate the rate for $K_L^o \to \pi^+\pi^-\gamma$ to that for $K_S^o \to \pi^+\pi^-\gamma$ or to that for $K_L^o \to \pi^o\pi^o\gamma$? The answer is no. The $K_S^o \to \pi^+\pi^-\gamma$ almost certainly goes predominantly by inner bremsstrahlung which is CP-conserving for this decay. The $K_L^o \to \pi^o\pi^o\gamma$ has no inner bremsstrahlung and no dipole transition. The latter is forbidden since conservation of angular momentum demands that the two pions be in an $\ell = 1$ state, and this is forbidden by Bose statistics. The dominant mechanism for $K_L^o \to \pi^o\pi^o\gamma$ is thus expected to be the electric quadrupole transition.

However, it is possible to relate our measurement to the K^+ and K^- radiative decays. The Cline extension of the $\Delta I = 1/2$ rule does give us the possibility of making a prediction from our result. According to Eq. (2) in Chapter II, $R_2(M1) = R_+(M1)$ where $R_2(M1)$ is the magnetic dipole contribution to $K_2^o \to \pi^+\pi^-\gamma$ and $R_+(M1)$ is the magnetic dipole contribution to $K^+ \to \pi^+\pi^-\gamma$. Using our upper limit, one obtains

$$R_+(M1) \leqslant 7.5 \times 10^3 \text{ sec}^{-1}$$

Since the magnetic dipole contribution to the K^+ decay is incoherent with the electric dipole and inner bremsstrahlung, the prediction above is for the total M1 contribution to the rate. Cline and Fry[36] report the rate $(K^+ \to \pi^+\pi^o\gamma) = (1.8 \pm 0.6) \times 10^4 \text{ sec}^{-1}$ for the π^+ energy between 55-80 MeV. Our predicted upper limit for magnetic dipole emission in this energy region is

$$R_+(M1) \leqslant 3.0 \times 10^3 \text{ sec}^{-1}$$

The K^+ - K^- radiative decays are of particular interest at the moment because a large CP-violation could manifest itself either as an asymmetry between K^+ and K^- Dalitz plots[37] or as a difference in the partial rates.[38] These effects, if they exist, result from interference between the inner bremsstrahlung and E1 amplitudes. The presence of magnet dipole emission will only tend to mask the effects.

Our estimate from Cline's hypothesis and our experiment is rather encouraging to a search for CP violation in the K^+- K^- radiative decay modes since it predicts an upper limit on the M1 contribution of less than 1/6 of the observed rate. The fruitfulness of such a search depends on the correctness of Cline and Fry's analysis that the anomalous energy pions in their experiment were associated with radiative decays. Actually the high energy gamma rays have not yet been seen.

LIST OF REFERENCES

1. J. H. Christenson, J. W. Cronin, V. L. Fitch, and R. Turlay, Phys. Rev. Letters 13, 138 (1964); A. Abashian, R. J. Abrams, D. W. Carpenter, G. P. Fisher, B.M.K. Nefkens, and J. H. Smith, Phys. Rev. Letters 13, 243 (1964).

2. J. M. Gaillard, F. Krienen, W. Galbraith, A. Hussri, M. R. Jane, N. H. Lipman, G. Manning, T. Ratcliffe, P. Day, A. G. Parham, B. T. Payne, A. C. Sherwood, H. Faissner, and H. Reithler, Phys. Rev. Letters 18, 20 (1967); J. W. Cronin, P. F. Kunz, W. S. Risk, and P. C. Wheeler, Phys. Rev. Letters 18, 25 (1967).

3. D. Dorfan, J. Enstrom, D. Raymond, M. Schwartz, S. Wojcicki, D. H. Miller, and M. Paciotti, Phys. Rev. Letters 19, 987 (1967). S. Bennett, D. Nygren, H. Saal, J. Steinberger, and J. Sunderland, Phys. Rev. Letters 19, 993 (1967).

4. T. D. Lee and L. Wolfenstein, Phys. Rev. 138, B1490 (1965); L. B. Okun (unpublished); J. Prentki and M. Veltman, Phys. Letters 15, 88 (1965).

5. J. Berstein, G. Feinberg, and T. D. Lee, Phys. Rev. 139, B1650 (1965).

6. Y. Ne'eman, Phys. Rev. Letters 13, 769 (1964).

7. L. Wolfenstein, Phys. Rev. Letters 13, 562 (1964).

8. T. D. Lee and C. S. Wu, Ann. Rev. Nucl. Sci. 16, 511 (1966).

9. L. M. Sehgal and L. Wolfenstein, Phys. Rev. 162, 1362 (1967).

10. D. Cline, Nuovo Cimento 36, 1055 (1965).

11. S. V. Pepper and Y. Ueda, Nuovo Cimento 33, 1614 (1964).

12. N. Cabibbo and R. Gatto, Phys. Rev. Letters 5, 382 (1960).

13. G. Feldman, P. Matthews, and A. Salam, Phys. Rev. 121, 302 (1961).

14. S. K. Bose, Phys. Letters 2, 92 (1962).

15. S. Oneda, S. Hori, M. Nakagawa, and Toyoda, Phys. Letters 2, 243 (1962).

16. S. Oneda, Y. S. Kim, and D. Korff, Phys. Rev. 136, B1064 (1964).

17. B. d'Espagnat, Phys. Letters 7, 209 (1963).

18. B. d'Espagnat, and Y. Villachon, Nuovo Cimento 33, 948 (1964).

19. S. Coleman and S. L. Glashow, Phys. Rev. 134, B671 (1964).

20. B. W. Lee, Phys. Rev. Letters 12, 83 (1964).

21. H. Sugawara, Nuovo Cimento 31, 635 (1964).

22. Y. Hara, Phys. Rev. Letters 12, 378 (1964).

23. B. Sakita, Phys. Rev. Letters 12, 379 (1964).

24. S. Okubo, Phys. Letters 8, 362 (1964).

25. C. S. Lai and B. L. Young, (to be published).

26. A. H. Rosenfeld, A. Barbaro-Galtieri, W. J. Podolsky, L. R. Price, Matts Roos, Paul Soding, W. J. Willis, and C. G. Wohl, Revs. Mod. Phys. 39, 1 (1967).

27. J. H. Knipp and G. E. Uhlenbeck, Physica 3, 425 (1936).

28. F. Block, Phys. Rev. 50, 272 (1936).

29. University of Illinois Modular Electronics Handbook (unpublished).

30. L. J. Verhey, Ph.D. Thesis, University of Illinois, 1967.

31. R. J. Abrams, Ph.D. Thesis, University of Illinois, 1966.

32. D. Hodges, "CHLOE, An Automatic Film Scanning Equipment, Hardware Reference Manual", Technical Memorandum No. 61, Applied Mathematics Division, Argonne National Laboratory (1963), unpublished.

33. R. Clark and W. F. Miller, "Computer Based Data Analysis Systems at Argonne", in Methods in Computational Physics, Vol. V, p. 47, Academic Press.

34. R. E. Mischke, Ph.D. Thesis, University of Illinois, 1966.

35. B. M. K. Nefkens, A. Abashian, R. J. Abrams, D. W. Carpenter, G. P. Fisher, and J. H. Smith, Phys. Rev. 157 (1967).

36. D. Cline and W. F. Fry, Phys. Rev. Letters 13, 101 (1959).

37. N. Christ, Phys. Rev. 159, 1292 (1967).

38. S. Barshay, Phys. Rev. Letters 18, 515 (1967).

VITA

Roy Cannon Thatcher was [redacted] He attended public schools in Ogden, where he graduated from Ogden High School in 1957. He attended Stanford University from 1957 to 1961 on a National Merit Scholarship. He received the degree of Bachelor of Science in Physics from there in 1961. In September of 1961 he became a student in the Physics Department of the University of Illinois, where he held teaching and research assistantships. He received the degree of Master of Science in Physics from the University of Illinois in June 1963.